The Geometry of Neuronal Recruitment

Jonathan Rubin* Amitabha Bose†

February 3, 2006

Abstract. We address the question of whether or not a periodic train of excitatory synaptic inputs recruits an excitable cell, such that it fires repeatedly, or does not recruit a cell, such that it fails to fire, possibly after some transient. In particular, we study the scenarios of one or two inputs per period; in the latter case, the degree of synchrony of the inputs is a crucial factor in recruitment. We establish rigorous geometric conditions that pinpoint the transition between recruitment and non-recruitment as the degree of synchrony between input pairs, or other input parameters, is varied. These conditions can be used to determine whether a particular temporal relation between periodic input pairs leads to recruitment or not and to prove, in certain parameter regimes, that recruitment can only occur when the inputs are sufficiently closely synchronized. The concepts in this paper are derived for both the integrate-and-fire neuron and the theta neuron models. In the former, the location in phase space of the unique fixed point of a relevant two-dimensional map determines firing, while in the latter, it is the existence or lack of existence of a fixed point of the map which does so. These results are discussed in the context of recruitment of cells into localized activity patterns.

Keywords. excitable neurons, integrate-and-fire model, theta model, synaptic input, geometric dynamical systems

1 Introduction

The activity of neurons is generally believed to encode and convey information through, for example, the firing rate, inter-spike interval or phase relationship between neurons. For a variety of reasons including issues of storage capacity, individual neurons (or sets of neurons) are believed to participate in multiple coding events. Thus neuronal codes cannot be hard wired into the brain and instead must be constructed in a transient

*Department of Mathematics and Center for the Neural Basis of Cognition, University of Pittsburgh, Pittsburgh, PA 15260; rubin@math.pitt.edu

†Department of Mathematical Sciences, New Jersey Institute of Technology, Newark, NJ 07102; bose@njit.edu

manner as a response to specific input signals. Examples where this type of idea may be utilized include progressive recall involving hippocampal place cells [14], working memory [20], and coincidence detection [2]. The construction of a neural code therefore relies on the ability of input stimuli to recruit appropriate silent neurons into the activity pattern that eventually forms the code. This observation leads to a very simple question: What detemines whether or not a stimulus recruits an excitable cell into an activity pattern?

While there is a considerable literature on the effect of periodic forcing, particularly smoothly varying forcing such as sinusoidal functions, on the behavior of oscillators, much of which builds on the paper of Keener et al. [9], there has been less work to date on the input-induced recruitment of excitable systems that are at rest in the absence of inputs [12], [18]. Pakdaman has studied the effect of continuous periodic forcing of a leaky integrate-and-fire neuron, under the assumption that the input integrates to zero over one period. By relating the dynamics to those of an appropriate circle map, he shows that the possible dynamic patterns are limited to periodic firing, quasiperiodic firing, nonchaotic aperiodic firing, or no firing whatsoever.

In this paper, we are primarily interested in exploring the conditions under which periodic, excitatory synaptic input can induce sustained firing of a post-synaptic neuron, in which case we shall say that the excitable cell has been recruited. We are interested in analyzing how the degree of synchrony of relevant inputs to an excitable neuron affects its recruitment. We develop a geometric perspective to establish criteria that distinguish between parameter sets that lead to recruitment or non-recruitment in some simple, yet representative, excitable systems. In particular, we derive a precise geometric criterion for the degree of synchrony between pairs of inputs needed for recruitment to occur.

In a prior paper, we studied the formation of bumps, or localized areas of sustained activity, in a network of coupled excitatory neurons [17]. We showed that stable localized solutions can occur, despite the absence of inhibition. The localized solutions are initiated by using a transient stimulus to induce a small number of cells to fire in synchrony. Since these cells are synchronized, they provide a relatively strong input to neighboring cells and can thus recruit them into the activity pattern. We showed, however, that the cells in the bump tend to desynchronize after the applied stimulus ends, which reduces the maximal synaptic input that they can provide to silent cells and which eventually may end the recruitment. In [17], we were able to give a cycle-by-cycle geometric criterion for whether or not a cell would be recruited. That is, we provided a condition that could be applied immediately after each synaptic input that a silent cell received to determine whether that cell would fire or not.

In this paper, we derive recruitment conditions that depend only on the nature of the input train, independent of initial conditions, which specify *a priori* whether a cell receiving this input train will be forced to fire in a sustained way or will be suppressed, possibly after an initial transient. The conditions are derived for both the integrate-

and-fire (IF) neuron model and the theta neuron model. In both cases, we derive a two-dimensional map which outputs the location in a relevant phase space of a cell after it receives a synaptic input. The map effectively reduces to a one-dimensional map since it uncouples in one of the two variables. In the IF case, we will show that the map always has a stable fixed point and that the location of this fixed point determines whether or not a cell is recruited. In the theta neuron case, we will show that the map need not have a fixed point, and that recruitment arises precisely when no fixed point exists. In [17], we worked with the Morris-Lecar model [11] for Type I cells, which feature a transition from silence to oscillations through a SNIC bifurcation [16]. We also considered the theta model, since it is a scalar equation that can be rigorously derived as a normal form for Type I neurons [10, 4, 8]. Thus, it is natural to consider the theta model here as well. We consider the IF model because it also possesses the Type I characteristic of onset of oscillations at zero frequency yet takes a particularly simple form; moreover, it allows for consideration of effects due to an imposed threshold. Despite their relative simplicity, we show that both of these models have rich geometric structures, which lead to some challenging mathematical questions. Interestingly, we show that significant qualitative differences arise in the geometries of the two models; further, although the location of the imposed threshold in the IF model does affect whether or not recruitment occurs for fixed parameter values, the imposition of threshold is not responsible for the contrast in the models' respective geometries.

The outline of the paper is as follows. Section 2 introduces the two different models. Section 3 is divided into 4 subsections. The first two, 3.1 and 3.2, deal with the IF model. In 3.1, we derive precise conditions on synaptic strength, period and decay rate that drive an IF cell to fire. These conditions are then generalized to the two input case in section 3.2. Sections 3.3 and 3.4 derive these concepts for the theta neuron model. In Section 4 we discuss the relationship of our results to the formation of localized regions of activity and to the progressive development of synchrony in cortical networks. We also discuss several open questions related to our work.

2 Model Equations

2.1 Integrate-and-Fire (IF) Neuron

We represent the dynamics of an IF neuron by the equation

$$v' = I - v \tag{1}$$

with a firing threshold v_{th} and a reset value v_r, which we without loss of generality set to $v = 1$ and $v = 0$, respectively, unless otherwise stated. Ignoring the threshold for a moment, note that $v = I$ is a stable fixed point. Therefore if $I > 1$, then any solution

trajectory with $v(0) < 1$ will at some time $t_1 > 0$ reach $v(t_1^-) = 1$. In the integrate-and-fire formalism, we reset $v(t_1^+) = 0$ and say that the neuron fired a spike at $t = t_1$. If the parameter $I < 1$, then $v(t) < 1$ for all t and the neuron never spikes. In this case, we say that the neuron is excitable. Excitable neurons require input to fire.

Fix $I < 1$ and consider the effect of periodic synaptic excitation on an IF neuron. We assume that an excitatory input, with instantaneous onset, arrives with period T. The equations of interest are:

$$\begin{aligned} v' &= I - v - g[v - E] \quad (2) \\ g' &= -\beta g, \quad (3) \end{aligned}$$

where $E > 1$ is the excitatory reversal potential and

$$g(nT^+) = g(nT^-) + k, \quad (4)$$

for $k > 0$ and $n = 1, 2, \ldots$ Equations (3-4) show that between inputs, the synaptic conductance g decays exponentially. But at the moment of a synaptic input, $g(t)$ is reset to $g(t) + k$. Note that $(I, 0)$ is a stable fixed point of (2-3).

2.2 Theta Neuron

The theta model is a canonical model for an oscillator in the neighborhood of a SNIC, or saddle-node on an invariant circle, bifurcation [7, 4, 8]. In the absence of input, the theta model takes the form

$$\theta' = 1 - \cos\theta + b(1 + \cos\theta), \quad (5)$$

where b is a parameter. For convenience, one identifies $\theta = -\pi$ with $\theta = \pi$ and thus considers $\theta \in S^1$. When the theta model is used to represent the dynamics of a neuron, the neuron is said to fire when θ increases through π. For $b < 0$, there exist two critical points of (5), given by $\theta_S = -\cos^{-1}(1+b)/(1-b) < 0$ and $\theta_U = \cos^{-1}(1+b)/(1-b) > 0$. The first is stable, while the second is unstable.

If a theta neuron receives excitatory input of the form discussed for the IF neuron, the governing equations become

$$\begin{aligned} \theta' &= 1 - \cos\theta + (b+g)(1 + \cos\theta), \\ g' &= -\beta g. \end{aligned} \quad (6)$$

As previously, equation (4) implements the arrival of each new input, when the input has period T. Critical points of equation (6) are $(\theta_S, 0), (\theta_U, 0)$. The zeros of the θ equation alone, however, depend on the level of input impinging on the theta neuron.

For $b < 0$ and $g > 0$ sufficiently small, there are two values of θ for which $\theta' = 0$ holds. As g increases, with $b < 0$ fixed, these values approach each other, until they meet at $(\theta, g) = (0, -b)$. Thus, the θ-nullcline forms an arc that extends from $(\theta_S, 0)$ up to $(0, -b)$ and back down to $(\theta_U, 0)$ in the (θ, g) phase plane.

3 Results

3.1 IF model - single input

Let c_1 be an excitable IF neuron, modeled by equations (2-4), which is subjected to periodic excitatory input of period T. Fix the parameters $I < 1$ and $E > 1$. If the synaptic input is such that c_1 fires repetitively, we say that c_1 has been recruited. We note that the sustained firing of c_1 is an important aspect of the definition of recruitment. For example, if c_1 is made to fire transiently several times, but eventually becomes quiescent, we will say that it has not been recruited. To be precise, we define recruitment by the condition that for every positive integer N, there exists an integer $n > N$ such that that the neuron fires during the time interval $[t_n, t_{n+1})$, where t_n is the onset time of the nth input. We shall answer the following question. What are the conditions on β, k and T such that c_1 is guaranteed to be recruited? The answer to this question appears to be intuitively clear. For example, if T is small and the reset value k is large enough (frequent large input), then c_1 should be recruited. Alternatively, if k is small and β is too large (small input that decays quickly), then c_1 should not be recruited. In this section, we will make these answers analytically and geometrically precise.

The v nullcline is found by setting the right-hand side of (2) equal to 0. This yields a curve

$$g = \frac{v - I}{E - v} \text{ for } v < E \tag{7}$$

in the $v - g$ phase plane. Note that this curve has a vertical asymptote at $v = E$, crosses the positive v axis at $v = I$, has positive slope ($dg/dv > 0$) and is concave up ($d^2g/dv^2 > 0$). On the v nullcline, since $v' = 0$ and $g' < 0$, the vector field points down. In the absence of input, all trajectories will converge to the stable critical point at $(I, 0)$.

We next define a map which will be used to track the behavior of trajectories in the $v-g$ phase plane. The input to c_1 arrives periodically every T time units. Thus we define $P(v(0^+), g(0^+)) = (v(T^+), g(T^+))$. This map takes an initial condition $(v(0^+), g(0^+))$ and returns the position of the variables at time T^+ after the reset due to synaptic input. Note that only g is reset; $v(0) = v(0^+)$ and $v(T) = v(T^+)$. We are interested in fixed points of the map P.

Let us first consider the behavior of the synaptic variable g. The dynamics of g decouple from those of v and can thus be understood independently. Define $\Delta g =$

$g(T^+) - g(0^+)$. Suppose $g(0^+) = g_0$. Solving (3), $g(T^-) = g_0 \exp(-\beta T)$. After the synaptic reset, using (4) and enforcing the fixed point condition $g(T^+) = g(0^+)$, we obtain the unique value $g_0 = g^*$ for which $\Delta g = 0$,

$$g^* = \frac{k}{1 - e^{-\beta T}}. \tag{8}$$

It follows from (8) that $g^* \to \infty$ as $k \to \infty$ or $T \to 0$ or $\beta \to 0$. Note that since we can solve for the value g^* independently of v, the map P effectively reduces to a one-dimensional map.

We next show how $v(t)$ changes over the time interval $[0, T]$. Let us ignore the threshold $v = 1$ for a moment. Then the region $I \le v \le E$ of the $v - g$ phase plane is positively invariant. In particular, if $v(0) = I$, then the fact that $v' > 0$ along $v = I$ yields $v(T) > v(0)$. Similarly, if $v(0) = E$, then the fact that $v' < 0$ on $v = E$ yields $v(T) < v(0)$. Thus, for each fixed $g > 0$, by the intermediate value theorem, there exists $v^* \in (I, E)$ such that if $v(0) = v^*$, then $v(T) = v^*$.

To show uniqueness of v^* for each g, we explicitly calculate its value using (2-3). Rewriting (2) and substituting $g(t) = g_0 \exp(-\beta t)$, we obtain the linear first order equation

$$v' + (1 + g_0 e^{-\beta t})v = I + g_0 e^{-\beta t} E.$$

Using an integrating factor and letting $E_1 = E - I$, we rewrite this as

$$\begin{aligned} v(t)e^{t - \frac{g_0}{\beta}e^{-\beta t}} &- v(0)e^{-g_0/\beta} \\ &= \int_0^t \left\{ I[1 + g_0 e^{-\beta s}] e^{s - \frac{g_0}{\beta}e^{-\beta s}} + g_0 e^{-\beta s} E_1 e^{s - \frac{g_0}{\beta}e^{-\beta s}} \right\} ds \\ &= I[e^{t - \frac{g_0}{\beta}e^{-\beta t}} - e^{-g_0/\beta}] + \int_0^t g_0 e^{-\beta s} E_1 e^{s - \frac{g_0}{\beta}e^{-\beta s}} \, ds. \end{aligned}$$

Thus if after a time T we want $v(T) = v(0) \doteq v^*$, we find that

$$v^*[e^{T - \frac{g_0}{\beta}e^{-\beta T}} - e^{-g_0/\beta}] = I[e^{T - \frac{g_0}{\beta}e^{-\beta T}} - e^{-g_0/\beta}] + \int_0^T g_0 e^{-\beta s} E_1 e^{s - \frac{g_0}{\beta}e^{-\beta s}} \, ds.$$

This can be written more compactly as

$$v^*(g, T) = I + \frac{F(g, T)}{K(g, T)}, \tag{9}$$

where

$$F(g, T) = \int_0^T g e^{-\beta s} E_1 e^{(s - \frac{g}{\beta}e^{-\beta s})} \, ds, \tag{10}$$

$$K(g, T) = e^{T - \frac{g}{\beta}e^{-\beta T}} - e^{-g/\beta}. \tag{11}$$

For fixed T, define $\Delta v = v(T) - v(0)$. Omitting explicit representation of its dependence on T (and on β), we note that the curve $v = v^*(g)$ is precisely the set of points in the $v-g$ phase that satisfy $\Delta v = 0$. Let us elucidate some of the properties of $v^*(g)$. First, note that $v^*(0) = I$ since $(I, 0)$ is a critical point of (2-3). Indeed, $v^*(g) \to I$ as $g \to 0$ because in this limit, $K(g,T) \to \exp(T) - 1$ while $F(g,T) \to 0$. Next, $v^*(g)$ must lie to the left of the v nullcline since $v' < 0$ below and to the right of the v nullcline and trajectories can only pass through it with $g' < 0$. Further, as $T \to \infty, v^*(g) \to I$, since $F(g,T) \leq E_1 g \int_0^T e^{(1-\beta)s}\, ds$, such that $F(g,T)/K(g,T) \to 0$ as $T \to \infty$. This corresponds to the fact that given a sufficiently long time, all trajectories approach arbitrarily close to $(I, 0)$, which means that $v_0 \approx I$ will be required to achieve $\Delta v = 0$ with large T.

We now establish two additional useful properties of $v^*(g)$.

Lemma 3.1 *The curve $v = v^*(g)$ converges to the v-nullcline as $g \to \infty$.*

Proof: As noted above, for each g, $v^*(g)$ lies to the left of the v-nullcline. This gives an upper bound of $v^*(g) < E$ as $g \to \infty$, based on solving equation (7) for v as a function of g. Similarly, $v^*(g) > I$ for all g. Since $v^*(g)$ is given by the formula $v^*(g) = I + F/K$ in equation (9), we will complete the proof by showing that $\partial(F/K)/\partial g \to 0$ as $g \to \infty$, which implies that $v^*(g)$ converges, and then showing that $v^*(g)$ cannot converge to any value strictly less than E. We omit explicit dependence on T in the following arguments.

Clearly, the sign of $\partial(F/K)/\partial g$ matches that of $L(g) \doteq (F'(g)K(g) - F(g)K'(g))/E_1$. A direct calculation, using (10),(11), gives

$$\begin{aligned} L(g) = \; & \tfrac{g}{\beta} \exp\left(\int_0^t (e^{-\beta s})^2 e^{(s - \frac{g}{\beta}e^{-\beta s})}\, ds\right)(e^{-g/\beta} - 1) + \left(\int_0^t e^{-\beta s} e^{(s - \frac{g}{\beta}e^{-\beta s})}\, ds\right) \cdot \\ & \left((\tfrac{g}{\beta}e^{-\beta t} + 1)e^{(t - \frac{g}{\beta}e^{-\beta t})} - (1 + g/\beta)e^{-g/\beta}\right) \to 0 \text{ as } g \to \infty, \end{aligned}$$

as desired.

Now, suppose that there exists G such that $F/K \leq B < E_1$ for all $g \geq G$, and let $\delta = E_1 - B > 0$. Note that points on the v-nullcline take the form $(v_n(g), g)$, where

$$v_n(g) \doteq \frac{I + Eg}{1 + g}.$$

Under the flow of (2),(3), trajectories $(v(t), g(t))$ originating from these points lie to the right of the v-nullcline, with $v(t) > v_n(g(t))$ for all positive time. Further, since $v_n(g) \to E$ as $g \to \infty$, there exists $\tilde{G} \geq G$ sufficiently large such that $v_n(g_0 e^{-\beta T}) > E - \delta/2$ for all $g_0 \geq \tilde{G}$. Now, the trajectory $(v(t), g(t))$ originating at $(v^*(g_0), g_0)$ must reach the v-nullcline within time T, since by definition of the function $v^*(g)$,

$$v(T) = v^*(g_0), \tag{12}$$

which requires $dv/dt < 0$ for some $t \in (0,T)$. Hence, we have $v(T) > E - \delta/2$, since $g_0 \geq \tilde{G}$, but $E - \delta/2 = B + I + \delta/2 > B + I$. This yields a contradiction to equation (12), however, because $g_0 \geq G$ implies $v^*(g_0) \leq B + I$. □

Remark 3.2 One can also establish the bound $v^*(g) < E$ analytically by computing that $F/K \leq E_1$ for all g, such that $v^* = I + F/K \leq I + (E - I) = E$ for all g. We omit the details here.

Lemma 3.3 *For any fixed $g > 0$, v^* is a monotone decreasing function of T.*

Proof: The lemma will be established by showing that $\partial v^*(g,T)/\partial T < 0$, where $v^*(g,T)$ is given by equation (9). Let

$$f(t) = \exp(t - \frac{g}{\beta}e^{-\beta t}) > 0. \tag{13}$$

Differentiation of equations (10) and (11), using $'$ now to denote differentiation with respect to T, yields

$$D(T) \doteq \frac{F'(T)K(T) - F(T)K'(T)}{E_1 g f(T)} = e^{-\beta T}(f(T) - e^{-g/\beta}) - \left(\int_0^T e^{-\beta s} f(s)\, ds\right)(1 + g e^{-\beta T}), \tag{14}$$

where we have neglected explicit representation of the g-dependence of the relevant functions. Note that the sign of $\partial v^*(g,T)/\partial T$ is given by the sign of $D(T)$, since the denominator of $D(T)$ is positive. Upon further differentiation, we obtain

$$\begin{array}{rcl} D'(T) & = & \beta e^{-\beta T}\left[-(f(T) - e^{-g/\beta}) + g\int_0^T e^{-\beta s} f(s)\, ds,\right] \\ D''(T) & = & \beta e^{-\beta T}\left[\beta(f(T) - e^{-g/\beta}) - f(T) - \beta g \int_0^T e^{-\beta s} f(s)\, ds\right] \end{array} \tag{15}$$

Equations (13), (14), (15) give $D(0) = 0, D'(0) = 0, D''(0) = -\beta e^{-g/\beta} < 0$. Further, suppose that $D(T) = 0$ for some $T > 0$. In this case, equations (14), (15) imply that $D'(T) = -\beta \int_0^T e^{-\beta s} f(s)\, ds < 0$. Hence, D cannot become nonnegative for positive T, and it follows that $\partial v^*(g,T)/\partial T < 0$ for all positive T, as desired. □

Consider again the map $P(v(0^+), g(0^+)) = (v(T^+), g(T^+))$. The unique fixed point of this map, (v^*, g^*), occurs when the line $g = g^*$ intersects the curve $v = v^*(g)$. From the construction of the map, it is clear that (in the absence of the threshold) the fixed point is globally attracting. Therefore, if $v^*(g^*) > 1$, then clearly c_1 is recruited into the activity pattern. By Lemma 3.1, for all other parameters fixed, there exists k sufficiently large such that $v^*(g^*) > 1$ occurs, so sufficiently strong inputs lead to recruitment. However, $v^* > 1$ is not a necessary condition for recruitment. To see this,

denote by A the point at which the line $v = 1$ intersects the v nullcline, i.e. the point $(v, g) = (1, \frac{1-I}{E-1})$. Let Γ denote the forward and backward trajectory through A. Follow A backward in time under the flow of (2),(3) for a time T. Denote this new point B and denote the trajectory connecting the points A and B by Γ_T. If we consider points lying on the line $v = 1$ with $g > \frac{1-I}{E-1}$ and follow these points backward in time for time T, we obtain a curve, which we denote $v = h(g)$, that has negative slope in the $v - g$ phase plane and terminates at the point B. Finally, by ES, denote the open region bounded to the left and below by the union of the curves $h(g)$ and Γ_T and to the right by the line $v = 1$. We call ES an exit set because any trajectory with initial conditions in it lies less than T away from the threshold $v = 1$. Thus any such trajectory will fire before the next synaptic input and then be reset. Figure 1A illustrates the relations, in the (v, g) phase plane, of the objects described here.

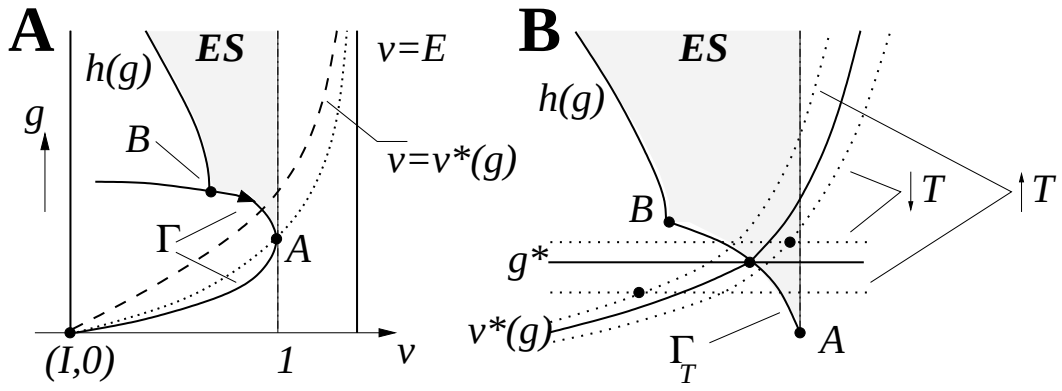

Figure 1: The (v, g)-phase space for the IF neuron with synaptic decay. A) Some relevant structures as discussed in the text; in particular, the dashed curve is $v^*(g)$ and the dotted curve is the v-nullcline. Γ_T, the subset of Γ between B and A, is not labelled here. Note that if an input places a cell into the exit set ES, then the cell will fire, by crossing the threshold $\{v = 1\}$ (dash-dotted vertical line), before the next input arrives. B) A zoomed view of ES. The solid curves depict $h(g), \Gamma_T$, as well as the curves $\{v = v^*(g)\}$ and $\{g = g^*\}$ for a special value of T such that $\{v = v^*(g)\} \cap \{g = g^*\}$ lies on the boundary of ES. Starting from this fixed T, the intersection moves into ES as T is decreased and out of ES as T is increased, as discussed in the text. The solid dots, other than the ones indicating the endpoints A, B of Γ_T, label intersection points corresponding to each of these three scenarios.

Consider now the relationship between the fixed point (v^*, g^*) of the map P and the set ES. If the fixed point lies in ES, then all trajectories will eventually enter ES since the fixed point is attracting. Once a trajectory enters ES, it will be forced to leave ES through the boundary $v = 1$. Thus if the parameters are such that the

fixed point lies in ES, then the neuron c_1 will fire repeatedly and therefore be recruited. Alternatively, if the fixed point does not lie in ES, then c_1 will not be recruited. In this case, depending on the initial conditions, a trajectory may fire several times, but eventually it is attracted to the fixed point that lies outside of ES. In summary, cell c_1 will be recruited if (v^*, g^*) lies in ES and will not be recruited if (v^*, g^*) lies outside of the closure of ES. Transitions between recruitment and non-recruitment occur at parameter values for which (v^*, g^*) lies on the boundary of ES, as shown in Figure 1B.

To analyze such transitions, we next discuss the relationship between the curves $v^*(g)$, Γ and $h(g)$. The key result here is Lemma 3.4.

Lemma 3.4 *$v^*(g) \cap \{\Gamma \cup h(g)\}$ consists of a single point lying in Γ_T.*

Proof: Based on slopes, $v^*(g)$ must intersect the union of Γ and $h(g)$. By definition, if $(v(0), g(0)) \in v^*(g)$ then $v(T) = v(0)$. But if $v(0) \in h(g)$, then $v(T) = 1 > v(0)$, a contradiction. Similarly, if $v(0) \in \Gamma \setminus \Gamma_T$ above the v-nullcline, then $v'(t) > 0$ for all $t \in [0, T]$ and $v(T) > v(0)$. Finally, if $v(0) \in \Gamma \setminus \Gamma_T$ below the v-nullcline, then $v'(t) < 0$ for all $t \in [0, T]$, and $v(T) < v(0)$. Therefore, $v^*(g)$ instead must intersect Γ_T. □

Based on this observation, consider parameter values for which $(v^*, g^*) \in \Gamma$. If T increases, corresponding to an increased input period, then the line $g = g^*$ moves to a smaller g value, while the curve $v^*(g, T)$ becomes more negative for each g, by Lemma 3.3. Thus, the intersection $(v^*(g^*, T), g^*)$ of these structures, for the increased T, occurs outside of ES, as shown in Figure 1B, and c_1 will not be recruited. On the other hand, if T decreases, corresponding to a decreased input period, then g^* grows, and $v^*(g, T)$ is larger for each g, again by Lemma 3.3, as also shown in Figure 1B. As a result, $(v^*(g^*, T), g^*)$ lies inside of ES, or possibly even to the right of $\{v = 1\}$, and c_1 will be recruited. In summary, the above analysis yields the following theorem.

Theorem 3.5 *For fixed β, k, there exists T_c such that c_1 is recruited by a periodic excitatory input of size k and period T if $T < T_c$, and c_1 is not recruited by this input if $T > T_c$. The value T_c is determined by the condition $(v^*(g^*(T_c), T_c), g^*(T_c)) \in \Gamma$.*

3.2 IF model - 2 inputs

Next, we consider how to generalize the above analysis to the case of two distinct inputs per period. For simplicity, we focus on two inputs of identical size. There are several possibilities that arise concerning the recruitment of c_1. For example, it is possible that either or both of the inputs are sufficiently strong and frequent to individually recruit c_1. We shall not directly consider these cases, as the single input analysis above is sufficient to describe the recruitment process there. Instead, we shall focus on the following

question. If neither input by itself is able to recruit c_1, will both inputs acting together be able to do so, and how does this depend on the relative timing of the two inputs? Asked in a different way, what degree of synchrony between the inputs is necessary to recruit c_1?

Assume that c_1 receives two distinct inputs, each of period $2T$. One input arrives at $t = 0, 2T, 4T, \ldots$ and the other at times $t = \Delta t, 2T+\Delta t, 4T+\Delta t, \ldots$ where $T \leq \Delta t \leq 2T$ (by symmetry we only need vary Δt over half the period). If $\Delta t = T$, then the inputs are maximally out-of-phase or maximally asynchronous. If $\Delta t = 2T$, then the inputs are completely synchronous. Note that these two situations are subcases of the single input analysis where the period is T and $2T$, respectively. In this section, we develop a geometric criterion that determines whether a pair of periodic inputs of given timing and magnitude will lead to recruitment or not, independent of the initial conditions of the cell receiving them. This criterion will arise as a natural generalization of results obtained for the single input case. Subsequently, we present numerical examples that illustrate the structures involved in this criterion, for particular parameter choices. Finally, we prove results based on our geometric criterion that clarify further the recruitment process when parameters satisfy certain relations. More specifically, we will prove that, at least in certain cases, there exists a unique value $\Delta t_c \in (T, 2T)$ such that if $\Delta t \geq \Delta t_c$, then c_1 will be recruited. That is, c_1 will be recruited only if the inputs arrive sufficiently closely in time. Our geometric criterion identifies precisely how close is sufficient.

3.2.1 Geometric representation of recruitment for IF in the 2-input case

First, consider the generalization of $v^*(g)$ to $v^*_{\Delta t}(g)$, defined for each g as the value of v at which $v(0) = v(2T)$, noting that the trajectory is reset at $t = \Delta t$ from the position $(v(\Delta t), g(\Delta t))$ to $(v(\Delta t), g(\Delta t) + k)$.

Lemma 3.6 *$v^*_{\Delta t}(g)$ exists and is unique for each $g > 0$.*

Proof: Fix $g > 0$. We consider a map $P_{\Delta t}(v)$ defined on $v \in [I, E]$ by flowing (v, g) under equations (2),(3) for time Δt, resetting from $(v(\Delta t), g(\Delta t))$ to $(v(\Delta t), g(\Delta t) + k)$ at $t = \Delta t$, continuing the flow until time $2T$, and projecting to the v coordinate. ¿From equation (2), it is obvious that $P_{\Delta t}(I) > I$ and $P_{\Delta t}(E) < E$. Further, for two initial conditions (v_1, g), (v_2, g) with $v_1 > v_2$, equation (2) implies that $(v_1 - v_2)' = -(1 + g)(v_1 - v_2) < 0$. Hence, $P_{\Delta t}$ is a contracting map from $[I, E]$ into itself, with a unique fixed point, which we call $v^*_{\Delta t}(g)$. □

The curves $v^*_T(g)$ and $v^*_{2T}(g)$ can be determined from the single input result found in equation (9). By Lemma 3.3, $v^*_{2T}(g)$ lies to the left of $v^*_T(g)$. As $\Delta t \to 2T$, the curve $v^*_{\Delta t}(g)$ converges to v^*_{2T} since these curves are both constructed using the flow for time $2T$. Note that $v^*_{\Delta t}(g)$ *does not* converge to $v^*_T(g)$ as $\Delta t \to T$, however, as the latter curve

is constructed using the flow for T, based on the condition $v(T) = v(0)$, while $v^*_{\Delta t}(g)$ is constructed using two resets, based on $v(2T) = v(0)$. Instead, $v^*_{\Delta t}(g)$ converges as $\Delta t \to T$ to a curve, which we denote $v^*_{T\cup T}(g)$ and which is unique by the argument used in the proof of Lemma 3.6. This curve intersects $v^*_T(g)$ at the value $g = g^*$ calculated from (8) and has greater slope than $v^*_T(g)$ where the two curves intersect, as shown in Figure 2A. To see this, consider the map P_T applied to a point (v_T, g) on the curve $v^*_T(g)$, with trajectory $(v_T(t), g(t))$ up to time T, when reset occurs, as shown in Figure 2B. If $g < g^*$, then $g(T) + k > g(0)$, and by uniqueness, $P_T(v_T) > v_T$. Hence, $v^*_{T\cup T}(g)$ lies to the right of $v^*_T(g)$ for $g < g^*$. Similarly, $v^*_{T\cup T}(g)$ lies to the left of $v^*_T(g)$ for $g > g^*$.

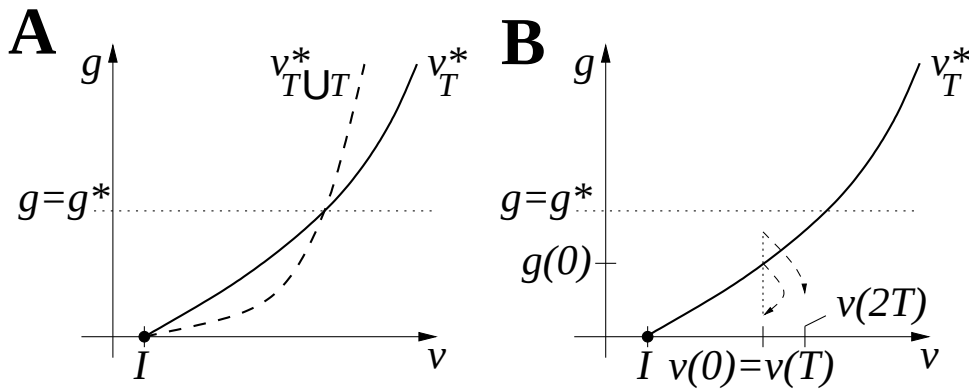

Figure 2: The curve $v^*_{T\cup T}(g)$ in relation to the curve v^*_T. A) Relative positions of the curves. B) Trajectories described in the argument showing that $v^*_{T\cup T}(g)$ lies to the right of v^*_T for $g < g^*$.

We are interested in where $v^*_{\Delta t}(g)$ lies relative to the curves $v^*_T(g)$, $v^*_{2T}(g)$ and $v^*_{T\cup T}(g)$. Denote by $(v_{\Delta t}(g), g)$ and $(v_{2T}(g), g)$ the points lying on the curves $v^*_{\Delta t}(g)$ and $v^*_{2T}(g)$, respectively. In particular, we have the following lemma.

Lemma 3.7 *The curve $v^*_{\Delta t}(g)$ lies to the right of the curve $v^*_{2T}(g)$; that is, for each $\Delta t \in [T, 2T)$ and each fixed g, $v_{\Delta t}(g) > v_{2T}(g)$.*

Proof: Choose a value g_0 and let $S = (v^*_{2T}(g_0), g_0)$ denote the intersection of $g = g_0$ and v^*_{2T}. Denote the trajectory through S by $\gamma_S = (v_S(t), g_S(t))$, such that $v_s(0) = v^*_{2T}(g_0)$, and note that if S is flowed forward a time $2T$, then by definition $v_S(2T) = v_S(0)$. Therefore, γ_S crosses through the v-nullcline at a unique time t_0 in $(0, 2T)$. Label the part of γ_S defined on time $[0, t_0)$ as γ^+_S. Now consider a trajectory $\gamma_{S'} = (v_{S'}(t), g_{S'}(t))$ defined by flowing S for time Δt (such that $(v_{S'}(t), g_{S'}(t)) = (v_S(t), g_S(t))$ for $t < \Delta t$), adding k to g, and then flowing the resulting point for an additional time $2T - \Delta t$. Let us first assume that $\Delta t > t_0$. It suffices to prove that $v_{S'}(2T) > v_S(2T) = v_S(0)$ if $\Delta t \in (T, 2T)$.

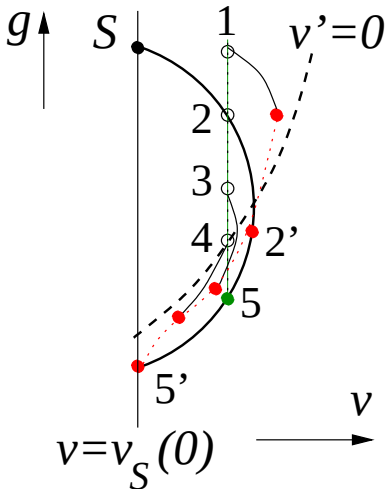

Figure 3: Proof that $v^*_{\Delta t}(g)$ lies to the right of $v_{2T}(g)$ for each g. The wide black curve is the trajectory γ_S, which satisfies $v_S(2T) = v_S(0)$. The green point on the curve denotes $(v_S(\Delta t), g_S(\Delta t))$, where g is to be incremented to form $\gamma_{S'}$. Different increment sizes k pick out different points on the dotted vertical line emanating from the green point. The figure illustrates five choices of k, labeled with numbers and, except for choice 5, with open circles. For choices 1, 3, and 4, the part of $\gamma_{S'}(t;k)$ defined on $(\Delta t, 2T)$ is given by a thin black curve, with the endpoint $\gamma_{S'}(2T;k)$ labeled in red. Note that number 2 corresponds to $k = k_+$ and number 5 corresponds to $k = 0$, both of which give $(v_{S'}(\Delta t^+), g_{S'}(\Delta t^+) \in \gamma_S$, such that the corresponding $\gamma_{S'}(t;k)$ are not visible; the corresponding endpoints are labeled 2' and 5', respectively. Number 4 corresponds to $k = k_0$, such that $(v_{S'}(\Delta t^+), g_{S'}(\Delta t^+))$ lies on the dashed v-nullcline. The trajectory $\gamma_{S'}(t;k)$ for choice 3 is squeezed between $\gamma_{S'}(t;k_0)$ and $\gamma_{S'}(t;k_+)$ for $t \in (\Delta t, 2T]$. A continuous curve $\gamma_{S'}(2T;k)$ (dotted red) passes through the red points shown and lies to the right of $v = v_S(0)$, the v-value at S. Note that the dotted red curve $\gamma_{S'}(2T;k)$ may intersect γ_S below $(v_S(\Delta t), g_S(\Delta t))$, rather than as shown here, but the same result holds in that case as well.

To do this, we fix Δt at an arbitrary value in $(T, 2T)$ and show that the desired inequality holds for all $k > 0$. Another way to think of this is that, if we plot the continuous curve $(v_{S'}(2T;k), g_{S'}(2T;k))$ in $v - g$ space, then it lies to the right of $\{v = v_S(0)\}$ for all $k > 0$; see Figure 3. In the following, we will use the notation $\gamma_{S'}(t;k)$ when we compare the positions at time t of the $\gamma_{S'}$ curves generated for different values of k, but for the most part we suppress explicit mention of dependence on k.

Start with k sufficiently large such that $v_{S'}(\Delta t)$ lies above γ_S^+, above the v-nullcline; see point 1 in Figure 3. After reset, $\gamma_{S'}$ must remain to the right of γ_S for $t \in (\Delta t, 2T)$ by uniqueness of solutions. Note that $g_{S'}(2T) > g_S(2T)$, since the point on $\gamma_{S'}$ after reset is $(v_{S'}(\Delta t^+), g_{S'}(\Delta t^+)) = g_0 \exp(-\beta \Delta t) + k$ and $g_{S'}(2T) = (g_0 \exp(-\beta \Delta t) + k) \exp(-\beta(2T - \Delta t)) > g_0 \exp(-2\beta T) = g_S(2T)$. Thus, the value of $v_{S'}(2T)$ in this case will be larger than $v_S(2T) = v_S(0)$.

The above case will occur for all k larger than the unique value $k_+ > 0$ for which $(v_{S'}(\Delta t^+), g_{S'}(\Delta t^+)) \in \gamma_S^+$. For $k = k_+$, shown as point 2 in Figure 3, $(v_{S'}(2T), g_{S'}(2T)) \in \gamma_S$ as well, and $g_{S'}(2T) > g_S(2T)$ again implies $v_{S'}(2T) > v_S$.

Next, consider the other extreme of small k. In particular, define k_0 such that $(v_{S'}(\Delta t^+), g_{S'}(\Delta t^+))$ lies below the v-nullcline if and only if $k < k_0$, and consider $k \in (0, k_0)$. Since $(v_{S'}(t), g_{S'}(t))$ lies closer to the v-nullcline than $(v_S(t), g_S(t))$ for all $t \in (\Delta t, 2T]$, following the reset, it follows that $0 > dv_{S'}(t)/dt > dv_S(t)/dt$ for all $t \in (\Delta t, 2T]$. Since $v_S'(\Delta t^+) = v_S(\Delta t^+)$, this inequality gives

$$v_{S'}(2T) > v_S(2T) = v_S(0),$$

with $v_{S'}(2T) \downarrow v_S(0)$ as $k \downarrow 0$. Since the vector field points down on the v-nullcline, a similar argument gives $v_{S'}(2T) > v_S(0)$ for $k = k_0$; see point 4 in Figure 3.

It remains to consider $k \in (k_0, k_+)$, for which $(v_{S'}(\Delta t^+), g_{S'}(\Delta t^+))$ lies between the v-nullcline and γ_S^+, as holds for point 3 in Figure 3. For each such k, $\gamma_{S'}(t; k)$ necessarily lies between $\gamma_{S'}(t; k_0)$ and $\gamma_{S'}(t; k_+)$ for all $t \in (\Delta t, 2T]$. Hence, $v_{S'}(2T; k) \in (v_{S'}(2T; k_0), v_{S'}(2T; k_+))$ for all $k \in (k_0, k_+)$, which completes the proof since $v_{S'}(2T; k_0) > v_S(0)$.

If $\Delta t < t_0$, then after the reset, $\gamma_{S'}$ is clearly to the right of γ_S and thus $v_{S'}(2T)$ will be larger than $v_S(0)$, as in the above case when k was large (point 1 in Figure 3); thus, the proof is complete. □

Remark 3.8 The curve $v^*_{\Delta t}(g)$ is not monotonic in Δt. In particular, as shown in Figure 7 below, $v^*_{\Delta t}(g)$ can lie to the right of $v^*_{T \cup T}$ for some values of $\Delta t \in (T, 2T)$.

Having understood which points lie on the curve $v^*_{\Delta t}(g)$, we now turn our attention to those points which are mapped back to their original g value after time $2T$, with resets of size k at $t = \Delta t \in [T, 2T]$ and at $t = 2T$. We can calculate the corresponding steady state level of g due to two inputs in the following way. Suppose an input arrives at $t = 0$ such that $g(0^+) = g_0$. If the next input arrives at Δt, then

$$g(\Delta t^+) = g_0 e^{-\beta \Delta t} + k.$$

Another input occurs at $t = 2T$ and after reset

$$g(2T^+) = (g_0 e^{-\beta \Delta t} + k) e^{-\beta(2T - \Delta t)} + k.$$

Now impose the periodicity condition that $g(2T^+) = g(0^+)$ to find g_0. Denote this value as

$$g^*_{\Delta t} = \frac{k[1 + e^{-\beta(2T-\Delta t)}]}{1 - e^{-2\beta T}}. \tag{16}$$

A straightforward calculation of $dg^*_{\Delta t}/d\Delta t$ shows that this derivative is always positive. Thus the steady state level of g increases as Δt increases from T to $2T$. This makes sense, as inputs that arrive closer in time should give a bigger synaptic kick than those that arrive farther apart. Moreover, for $\Delta t > T$, which we can always arrange by redefining which input occurs first in each cycle, direct calculation yields

$$\begin{cases} g(0^+) > g(\Delta t^+) > g(2T^+), & g > g_3, \\ g(0^+) > g(2T^+) > g(\Delta t^+), & g_3 > g > g_2, \\ g(2T^+) > g(0^+) > g(\Delta t^+), & g_2 > g > g_1, \\ g(2T^+) > g(\Delta t^+) > g(0^+), & g_1 > g. \end{cases}$$

Here, $g_3 > g_2 > g_1$ are given by

$$g_1 = \tfrac{k}{1-e^{-\beta\Delta t}}, \text{ derived from solving } g(\Delta t^+) = g(0^+),$$

$$g_2 = g^*_{\Delta t}, \text{ from equation (16)},$$

$$g_3 = \tfrac{ke^{-\beta(2T-\Delta t)}}{e^{-\beta\Delta t}-e^{-2\beta T}}, \text{ derived from solving } g(2T^+) = g(\Delta t^+).$$

By abuse of notation, let us now use $P_{\Delta t}$ to denote the full 2-dimensional time $2T$ return map, given by $P_{\Delta t}(v(0^+), g(0^+)) = (v(2T^+), g(2T^+))$, where $\Delta t \in [T, 2T]$ denotes the timing of the second input relative to the first. Based on Lemma 3.6, its proof, and equation (16), for each $\Delta t \in [T, 2T]$, there exists a unique fixed point of $P_{\Delta t}$, namely the point $(v^*_{\Delta t}, g^*_{\Delta t})$, and it is attracting. We emphasize that, based on the above calculation with $\Delta t > T$, $g^*_{\Delta t} > g_1$ always holds, which we will use below.

The main question to address is whether this fixed point lies in a region of recruitment or not. Answering this question requires us to determine the exit set for the 2-input case. In the previous section, we defined the exit set ES, which consisted of those initial conditions that cross or reach $\{v = 1\}$ under the time T flow. It was bounded by the curves Γ_T and $h(g)$. To generalize this to the 2-input case, define $\Gamma_{\Delta t}$ to be the curve formed by flowing the point A, given by $(v, g) = (1, (1 - I)/(E - 1))$, backward in time an amount $\Delta t \in [T, 2T]$. For any Δt, the right endpoint of $\Gamma_{\Delta t}$ is the point A. The left endpoint lies on the trajectory Γ and depends on Δt. In particular, when $\Delta t = T$, this endpoint is the point B as in the previous section. When $\Delta t = 2T$, the endpoint lies at a point C. In general, for any $\Delta t \in (T, 2T)$, the left endpoint lies between the points

B and C and tends to these points in the limits $\Delta t \to T$ and $\Delta t \to 2T$, respectively. For any $\Delta t \in [0, 2T]$, the curve $h(g)$ generalizes to a curve $h_{\Delta t}(g)$ which is defined by flowing the set of points along $v = 1$ for $g > (1-I)/(E-1)$ backward in time an amount Δt. Note that the family $h_{\Delta t}(g)$ moves left, away from $v = 1$, as Δt increases. For the 2-input case, we now define ES as the set of points bounded to the left by $h_{\Delta t}(g)$, below by $\Gamma_{\Delta t}$ and to the right by the line $v = 1$. Note that any initial condition starting within ES will clearly reach threshold $v = 1$ in a time less than Δt. However the set of points ES does not contain all points which cross or reach the threshold $v = 1$ under the time $2T$ flow (with synaptic reset at $t = \Delta t$). We denote that larger set of points by $\tilde{ES}$. The set $\tilde{ES}$ can be viewed as the union of two different subsets. One subset consists of all points lying above Γ that are within time $2T$ of $v = 1$, when reset is taken into account. The other subset consists of those points that, when flowed forward a time Δt, are reset above Γ and to the right of the curve $h_{2T-\Delta t}(g)$. Points that are reset in this way can cross threshold in time less than $2T - \Delta t$. In Appendix A, we provide a complete description of the set $\tilde{ES}$. However, as we will show below, it is the set ES, not $\tilde{ES}$, that is most relevant for recruitment in the 2-input case.

We are now in a position to determine the location of fixed points of the map $P_{\Delta t}$. There are a few important points in the v-g phase plane we must first identify. One is the point R. For each fixed k translate the part of Γ that lies above the v-nullcline, which terminates in point A, down by k units in the g-direction. Then set R as the unique point of intersection of the translated curve and Γ. Denote the coordinates of R by (v_R, g_R). Next let $\hat{R}_{\Delta t}$ be the point (on Γ) obtained by flowing R backward for time Δt. By this definition, if we start at $\hat{R}_{\Delta t}$, flow forward for time Δt to the point R, and then add k to the g-coordinate of R, then we obtain a point along Γ, which we label Q, with coordinates (v_Q, g_Q). We also define Γ^- to be the part of Γ lying below the v-nullcline, which contains R but not $\hat{R}_{\Delta t}$ and Q. Figure 4 illustrates the structures described here.

As discussed above, the return map will have a unique fixed point $(v^*_{\Delta t}(g), g^*_{\Delta t})$ for each $\Delta t \in (T, 2T)$. The following Lemma restricts where these fixed points may lie, explicitly showing that they cannot lie in $\tilde{ES} \setminus ES$.

Lemma 3.9 *For each $\Delta t \in [T, 2T]$, the map $P_{\Delta t}$ has no fixed points in $\tilde{ES} \setminus ES$.*

Proof: Recall that Γ_t denotes the part of Γ obtained by flowing A backward under (2)-(3) for time t and that ES is the set of points bounded to the left by $h_{\Delta t}(g)$, below by $\Gamma_{\Delta t}$, and to the right by the line $v = 1$. First, we characterize the location of points in $\tilde{ES} \setminus ES$. Note that the concatenated curves $h_{\Delta t}(g) \cup h_{2T-\Delta t}(g) \cup \Gamma$ partition the rest of the (v, g)-plane into four open components, as shown in Figure 5. Denote these components by C_1, which is bounded above and below by Γ and does not intersect $\{v = 1\}$, C_2, which contains all of $\{v = 1\}$ except $A \in \Gamma$ and which is positively invariant

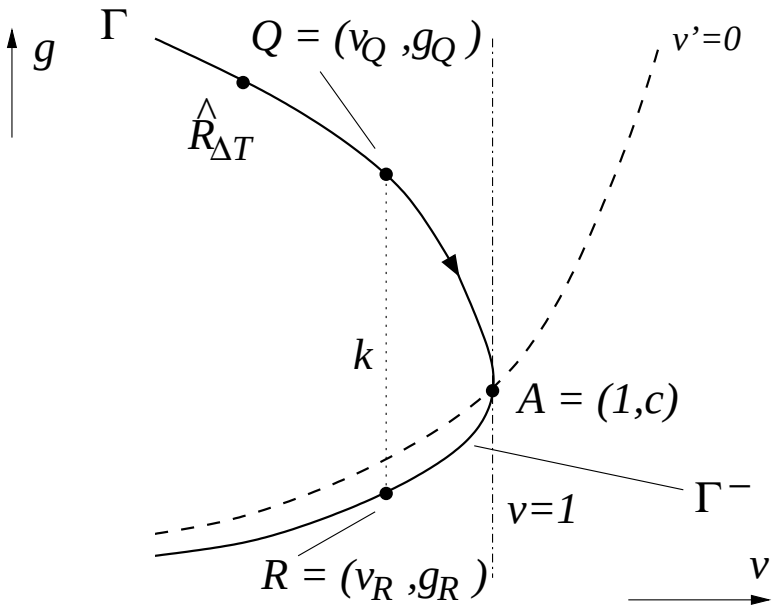

Figure 4: The unique trajectory Γ passes through the point A where the v-nullcline intersects $\{v = 1\}$; Γ^- is the part of Γ below the v-nullcline, while $\Gamma_{\Delta t}$ (not labeled here) is the part of Γ extending from $\hat{R}_{\Delta t}$ to A. The point $\hat{R}_{\Delta t}$ is carried to the point R by the flow in time Δt. Note that $c = (I-1)/(1-E)$ and that $v_Q = v_R, g_Q = g_R + k$.

under the flow of (2),(3) without reset, C_3, which lies between $h_{\Delta t}(g)$ and $h_{2T-\Delta t}(g)$ and is nonempty because $\Delta t > 2T - \Delta t$, and C_4, which lies above Γ and left of $h_{\Delta t}(g)$. We have $ES = C_2 \cup C_3$ while $\tilde{ES} \setminus ES \subset C_1 \cup C_4$.

Suppose that an arbitrary initial condition $(v(0), g(0))$ in $\tilde{ES} \setminus ES \cap C_1$ is a fixed point of $P_{\Delta t}$. As noted above, since this is a fixed point, $g(0) > g_1$; therefore, if this initial point is flowed for time Δt to $(v(\Delta t), g(\Delta t))$ and then reset, then

$$g(\Delta t) + k < g(0). \tag{17}$$

Now, since $(v(0), g(0))$ is a fixed point of $P_{\Delta t}$, the time $2T - \Delta t$ flow must carry $(v(\Delta t), g(\Delta t) + k)$ to $(v(0), g(0) - k)$. Further, $(v(0), g(0))$ has been selected to lie in $\tilde{ES}$, so the trajectory generated by this flow must cross $\{v = 1\}$. This is only possible if $(v(\Delta t), g(\Delta t) + k)$ lies to the right of $h_{2T-\Delta t}$ and above $\Gamma_{2T-\Delta t}$; that is, $(v(\Delta t), g(\Delta t) + k) \in C_2$. Since $g(\Delta t) + k < g(0)$ and the curves $h_{2T-\Delta t}, \Gamma_{2T-\Delta t}$ have negative slopes as functions of g, it follows that $v(\Delta t) > v(0)$, as illustrated in Figure 5.

Since $(v(\Delta t), g(\Delta t) + k) \in C_2$, the image of this point under the time $2T - \Delta t$ flow must remain in C_2. Initially, its v-component will increase, and later it will decrease

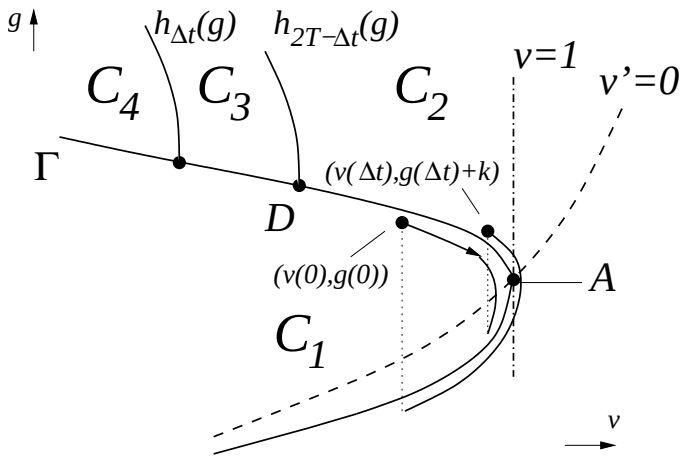

Figure 5: The curves $h_{\Delta t}(g), h_{2T-\Delta t}(g)$, and Γ partition the plane into four open components, C_1, C_2, C_3, C_4. If $P_{\Delta t}$ has a fixed point $(v(0), g(0))$ in $\tilde{ES}$ within component C_1, then after it flows for time Δt plus reset, it must lie in component C_2, as shown, since it lies in $\tilde{ES}$. To be a fixed point of $P_{\Delta t}$, the flow must return it to its original v-coordinate after its first reset, and then it will be reset again. But the two reset distances in g, shown by the two dotted lines, cannot be equal.

until it reaches $v(2T) = v(0)$. Let $\tau \in (0, 2T - \Delta t)$ denote the time such that $v(\Delta t + \tau) = v(\Delta t)$. Since the image of $(v(\Delta t), g(\Delta t) + k)$ lies in C_2 and $(v(\Delta t), g(\Delta t))$ lies in C_1, we have $g(\Delta t + \tau) < g(\Delta t)$. Hence, $g(2T) < g(\Delta t + \tau)$, from equation (3), yields

$$g(2T) < g(\Delta t). \tag{18}$$

Since $(v(0), g(0))$ is a fixed point of $P_{\Delta t}$, the equality $g(2T) + k = g(0)$ must hold. But inequalities (17), (18) yield

$$g(2T) + k < g(\Delta t) + k < g(0), \tag{19}$$

a contradiction.

Finally, $P_{\Delta t}$ has no fixed points in $\tilde{ES} \setminus ES \cap C_4$ by a similar argument. That is, if $(v(0), g(0)) \in \tilde{ES} \setminus ES \cap C_4$, then $(v(t), g(t))$ crosses $v = 1$ after time Δt. Hence, the inequalities in (19) again hold by the argument given above, again giving a contradiction. □

The next set of results gives more information on potential locations where the set of fixed points of $P_{\Delta t}$ may lie. Henceforth, we use the phrases "to the left (right) of" to refer to points in Γ that have larger (smaller) g-values and smaller (larger) v-values than those of other points, or sets of points, in Γ.

Lemma 3.10 *For $\Delta t \in [T, 2T]$, if $\hat{R}_{\Delta t}$ lies to the right of Q on Γ, then the fixed point $(v^*_{\Delta t}(g), g^*_{\Delta t})$ of $P_{\Delta t}$ lies in ES or has $v^*_{\Delta t} > 1$.*

Proof: Fix $\Delta t \in [T, 2T]$ and assume $\hat{R}_{\Delta t}$ lies to the right of Q. We will show that the fixed point $(v^*_{\Delta t}, g^*_{\Delta t})$ of $P_{\Delta t}$ has $v^*_{\Delta t} > v_Q$ and $g^*_{\Delta t} > g_Q$. Thus the fixed point will lie either in ES or to the right of $v = 1$. Recall that the fixed point is attracting. Further note that the g component of the time $2T$ map is monotone. Thus if $g(0) < g(2T^+)$, then $g(2nT^+) < g((2n+2)T^+) < g^*_{\Delta t}$ for all $n = 1, 2, 3, \ldots$.

Let $(v(0), g(0))$ lie at the point $\hat{R}_{\Delta t}$ lying to the right of Q. By definition, this point flows to R at time Δt, and is reset to the point Q. It then flows along Γ for another $2T - \Delta t$. Note that $(v(2T^-), g(2T^-)) \in \Gamma$, but $g(2T^-)$ is greater than g_R, the g value at the point R. Thus after reset, $(v(2T^+), g(2T^+)) \in ES$. In particular, $g(2T^-) > g_R$ implies $g(2T^+) = g(2T^-) + k > g_R + k = g_Q > g(0)$. The monotonicity in g then implies that $g^*_{\Delta t} > g_Q$.

The above argument also shows that $v(2T) > v_Q$. Since $v(2nT) \to v^*_{\Delta t}$ as $n \to \infty$, we need only show that the forward iterates $v(2nT)$ satisfy $v(2nT) > v_Q$ for each n. Consider the point $(v(2T), g(2T^+))$ flowed forward for time Δt. This trajectory must lie in C_2, and in particular, monotonicity gives $g(2T^- + \Delta t) > g_R$. Therefore $v(2T + \Delta t) > v_Q$ and $g(2T^+ + \Delta t) > g_Q$. So $(v(2T + \Delta t), g(2T^+ + \Delta t))$ lies in C_2 and $v(4T) > v_Q$ results. The same argument can be applied at each time $2nT$ to reach the conclusions of the Lemma. □.

Lemma 3.11 *If $\hat{R}_{\Delta t}$ lies to the left of Q, then any fixed point of $P_{\Delta t}$ on Γ lies between $\hat{R}_{\Delta t}$ and Q.*

Proof: If $(v(0), g(0)) \in \Gamma$ is a fixed point to the left of $\hat{R}_{\Delta t}$, then $(v(\Delta t), g(\Delta t) + k) \in C_2$, by the definition of $\hat{R}_{\Delta t}$. Hence, the argument in the proof of Lemma 3.9 gives a contradiction. If $(v(0), g(0)) \in \Gamma$ is a fixed point lying to the right of Q, then $(v(\Delta t), g(\Delta t) + k) \in C_1$, which is positively invariant between resets. Since $g(0) < g_Q$ and $(v(2T), g(2T^-)) \in C_1$, the condition $g(2T^-) + k = g(0)$ implies that $g(2T) + k < g_R$. Hence, $v(2T) < v_R = v_Q < v(0)$, contradicting the assumption that $(v(0), g(0))$ is a fixed point. □

Henceforth, let $\hat{\Gamma}_{\Delta t}$ denote the segment of Γ between $\hat{R}_{\Delta t}$ and Q, regardless of which of these points lies to the left of the other. For each Δt, the fixed point of $P_{\Delta t}$ may lie either in the part of C_1 bounded above by Γ and below by the v-nullcline, in which case recruitment fails; above Γ and to the right of $h_{\Delta t}(g)$, in which case recruitment occurs; or exactly on $\hat{\Gamma}_{\Delta t}$, if $\hat{R}_{\Delta t}$ lies to the left of Q. Since $g^*_{\Delta t}$ increases with Δt, it seems plausible to expect a progression from non-recruitment to recruitment as Δt increases from T to $2T$, with the transition occurring at some unique Δt for which the fixed

point of $P_{\Delta t}$ lies in $\hat{\Gamma}_{\Delta t}$. However, the change in $v^*_{\Delta t}$ with Δt may be non-monotone, so this progression is not guaranteed. Based on Lemma 3.11, if $g^*_{\Delta t}$ moves above $\hat{R}_{\Delta t}$ for some Δt, then $P_{\Delta t}$ cannot have a fixed point on Γ, and thus recruitment will be maintained if it has been achieved already; however, like $g^*_{\Delta t}$, the g-coordinate of $\hat{R}_{\Delta t}$ increases with Δt, so $\hat{R}_{\Delta t}$ could theoretically overtake $g^*_{\Delta t}$ as Δt increased further. In Appendix B, we present Lemma 5.1 and Lemma 5.2, which further refine this picture, and Figure 6 illustrates some of the possibilities that emerge. In the next subsection, we examine numerical examples and establish conditions that guarantee that a progression from non-recruitment to recruitment with increasing Δt does indeed occur.

3.2.2 Numerics for IF in the 2-input case

The results discussed above provide a strict criterion for a transition between non-recruitment and recruitment to occur. Specifically, such a transition will occur at a value Δt if and only if $P_{\Delta t}$ has a fixed point in $\hat{\Gamma}_{\Delta t} \subset \Gamma$, which is only possible if $\hat{R}_{\Delta t}$ is to the left of Q. Figure 7 shows a numerical example of how relevant structures evolve as Δt is increased; the simulations for this, and all other numerical figures in the paper, were performed using XPPAUT [5]. This figure was generated using equations (2),(3),(4) with $I = 1, E = 2, \beta = 0.5, k = 1, T = 4.25$ and various values of Δt, as listed in the caption, and also various thresholds for v (rather than $v = 1$), as discussed in the next paragraph. In the plot, each solid curve represents $v^*_{\Delta t}$ for some choice of Δt, with the exception of the black solid curve, which is v^*_T and is shown for comparison. The results show that as Δt is increased from T, $v^*_{\Delta t}$ moves away from $v^*_{T \cup T}$ in a non-monotone way, moving towards larger v-values at first and then coming back to smaller v-values, converging to v^*_{2T} as $\Delta t \uparrow 2T$. We observed a similar non-monotonicity for other parameter sets used.

Unlike $v^*_{\Delta t}$, the value $g^*_{\Delta t}$ increases monotonically with Δt, as can be seen from equation (16). The asterisk on each solid curve shows its intersection with $g = g^*_{\Delta t}$ for the corresponding value of Δt (note that $g^*_{\Delta t}$ for the Δt used for curve 5 is extremely close to g^*_{2T}). While the thick dashed red curve is the v-nullcline, the thin dashed black curves denote the position of the curve Γ for three different choices of threshold value for v, namely $v_{th} = 1.5, 1.55$, and 1.6. For $v_{th} = 1.5$ (leftmost dashed black curve in Figure 7), there is a unique value of Δt between 5.5 and 7 for which $P_{\Delta t}$ has a fixed point in Γ. Interestingly, this occurs for Δt sufficiently small such that $v^*_{\Delta t}$ is still increasing in Δt. For $v_{th} = 1.55$ (middle dashed black curve in Figure 7), the situation is more subtle. Our numerics indicate that there again is a unique Δt for which the fixed point of $P_{\Delta t}$ lies on Γ, but it occurs for larger Δt, for which $v^*_{\Delta t}$ is decreasing, and hence it is more difficult to discern whether it is truly locally unique. Finally, for $v_{th} = 1.6$ (rightmost dashed black curve in Figure 7), the fixed point of $P_{\Delta t}$ lies below Γ for all $\Delta t \in [T, 2T]$, and recruitment never occurs.

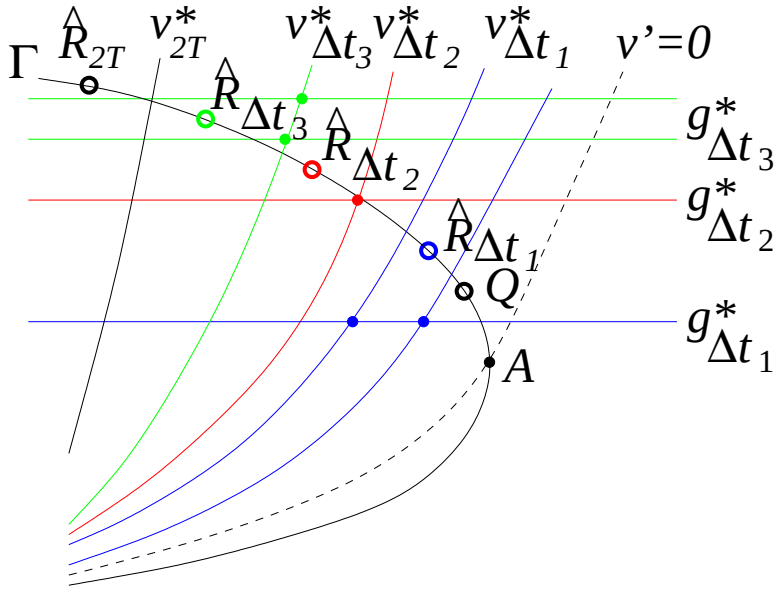

Figure 6: A possible progression of the fixed points of $P_{\Delta t}$ for $\Delta t_1 < \Delta t_2 < \Delta t_3$, all in $[T, 2T)$. All blue, red, and green objects correspond to $\Delta t = \Delta t_1, \Delta t_2, \Delta t_3$, respectively. Solid circles denote fixed points of $P_{\Delta t}$ for corresponding Δt, while the three slightly enlarged but hollow circles denote $\hat{R}_{\Delta t}$. For $\Delta t = \Delta t_1$, two different curves $v^*_{\Delta t_1}$ are shown to illustrate two different possible locations of this curve; for fixed parameters, only one such curve would exist; similarly, for $\Delta t = \Delta t_3$, two possible locations of $g^*_{\Delta t_3}$ are shown. Note that all v^* curves lie to the right of v^*_{2T}, by Lemma 3.7. When $\Delta t = \Delta t_1$ as shown, $v^*_{\Delta t_1}$ intersects Γ at $g > g^*_{\Delta t_1}$. Hence, this intersection may occur above or below $\hat{R}_{\Delta t_1}$, but must be to the left of Q; in either case, $v^*_{\Delta t_1} \cap g^*_{\Delta t_1}$ lies below Γ, outside of $\tilde{ES}$, and no recruitment occurs. When $\Delta t = \Delta t_2$ as shown, $v^*_{\Delta t_2} \cap g^*_{\Delta t_2}$ occurs exactly on Γ and to the right of $\hat{R}_{\Delta t_2}$ (i.e., on $\hat{\Gamma}_{\Delta t_2}$), by Lemma 3.9, corresponding to the boundary between recruitment and non-recruitment. When $\Delta t = \Delta t_3$ as shown, $v^*_{\Delta t_3} \cap g^*_{\Delta t_3}$ occurs above Γ, leading to recruitment. Since $v^*_{\Delta t_3} \cap \Gamma$ occurs below $g_{\Delta t_3}$, this intersection must lie to the right of $\hat{R}_{\Delta t_3}$ (i.e., on $\hat{\Gamma}_{\Delta t_3}$), by Lemma 5.1. Finally, note that $\hat{R}_{2T}$ must lie to the left of the point $v^*_{2T}(g) \cap \Gamma$, if recruitment occurs for $\Delta t = 2T$, by Lemma 5.2.

There are other ways to check the uniqueness of the transition point numerically, as an alternative to computing positions of fixed points of $P_{\Delta t}$ directly. For example, recall that for $P_{\Delta t}(v(0), g(0)) = (v(2T), g(2T^+))$, we define $\Delta v = v(2T) - v(0)$. For

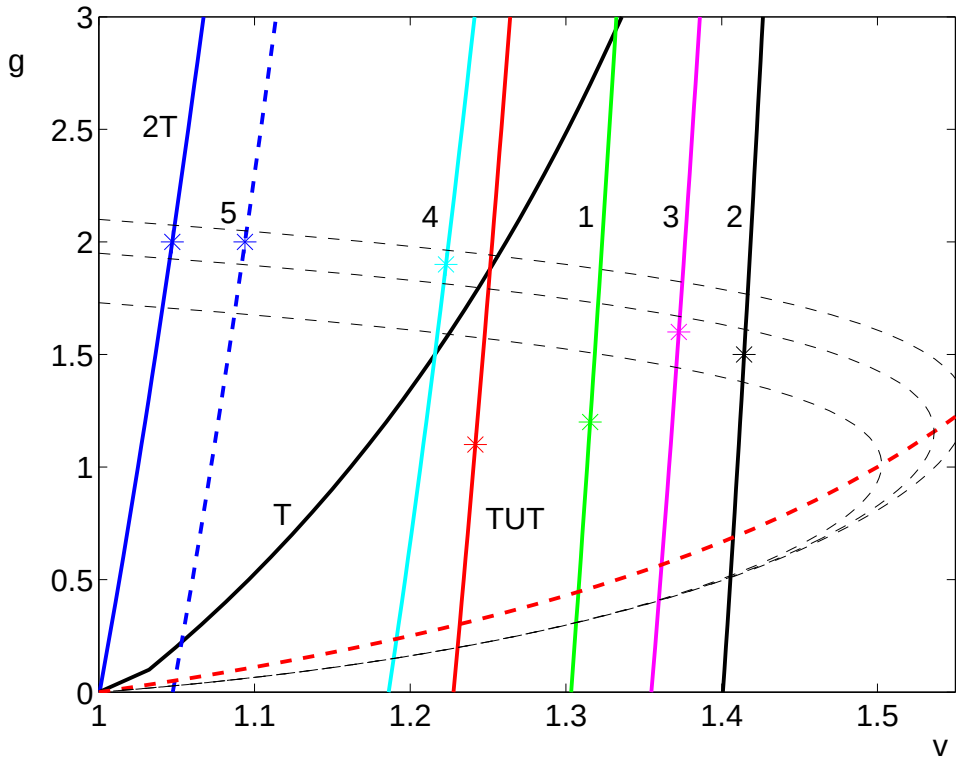

Figure 7: An example of the evolution of $v^*_{\Delta t}$ and $g^*_{\Delta t}$ with Δt, along with other relevant curves. The solid curves labeled with numbers correspond to $v^*_{\Delta t}$ with **1:** $\Delta t = 5.5$, **2:** $\Delta t = 7$, **3:** $\Delta t = 7.2$, **4:** $\Delta t = 8.25$, **5:** $\Delta t = 8.45$, which all lie in $(T, 2T) = (4.25, 8.5)$. The asterix on each curve denotes the position of the fixed points of $P_{\Delta t}$. All other parameter values are given in the text, where the other objects in the figure are also described.

each point on Γ, we can compute Δv. For each Δt, let $\Delta v(\Delta t)$ denote the value of Δv found by applying the map $P_{\Delta t}$ to the unique intersection between the line $g = g^*_{\Delta t}$ and Γ. Since recruitment transitions correspond precisely to fixed points of $P_{\Delta t}$ in Γ, we have $\Delta v(\Delta t) = 0$ if and only if a transition occurs at Δt. Thus, given that a transition occurs, its uniqueness is guaranteed if we can show that $d(\Delta v)/d(\Delta t) > 0$ for all Δt. We have checked this carefully for various parameter sets, and we have always found that this inequality holds. Figure 8 shows two examples.

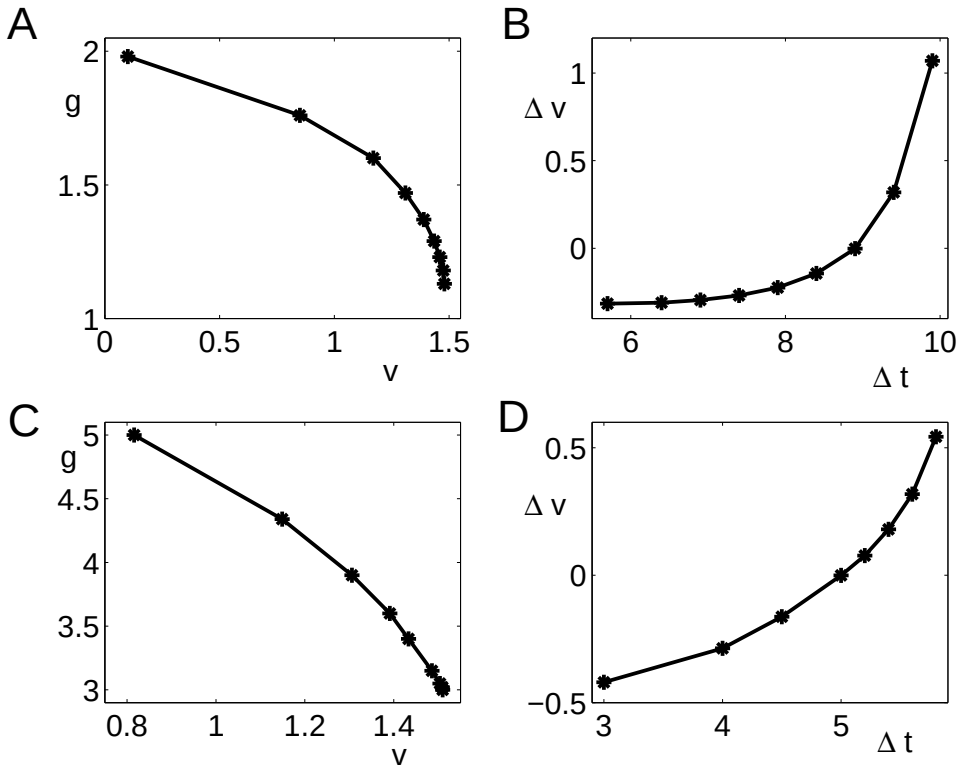

Figure 8: Change in Δv with Δt along Γ. A,B) $\beta = 0.5, T = 5, k = 1$. C,D) $\beta = 2, T = 3, k = 3$. Both A) and C) show points sampled along Γ for the associated parameter values. Each sampled point represents $g^*_{\Delta t}$ intersected with Γ for a particular value of Δt. These values are used in plots B) and D), which show the value of Δv found by implementing the map $P_{\Delta t}$ from the corresponding initial point on Γ, for each Δt used in A) and C), respectively. The slopes of these curves, $d(\Delta v)/d(\Delta t)$, are unambiguously positive. The unique Δt for which the fixed point of $P_{\Delta t}$ lies on Γ is given by the Δt value for which $\Delta v(\Delta t) = 0$, which are approximately $\Delta t = 8.9$ in A,B) and $\Delta t = 5.0$ in C,D).

3.2.3 Refinement of the recruitment picture in particular parameter regimes

We will now use equation (16) to derive conditions on non-recruitment and recruitment for the boundary cases when $\Delta t = T$ and $2T$ respectively. This will allow us to prove the following lemma.

Lemma 3.12 *Fix $k < (1 - I)/2(E - 1)$. Then for E sufficiently large or β sufficiently*

small, there exists an interval of T values $[T_{lo}, T_{hi}]$ such that if $T \in [T_{lo}, T_{hi}]$, then recruitment occurs for $\Delta t = 2T$ and fails for $\Delta t = T$.

Proof: As seen in subsection 3.2.1, for fixed T, as Δt varies, all transitions between recruitment and non-recruitment must correspond to the existence of a fixed point $(v^*_{\Delta t}, g^*_{\Delta t})$ of $P_{\Delta t}$ on $\hat{\Gamma}_{\Delta t}$, the subset of Γ between $\hat{R}_{\Delta t}$ and Q, for a value of Δt for which $\hat{R}_{\Delta t}$ lies to the left of Q. Let $\tilde{g}$ denote the g-value of the unique intersection point of v^*_{2T} with Γ and recall that the g-value of the point Q is denoted g_Q. Since Lemma 3.7 shows that $v^*_{\Delta t}$ lies to the right of v^*_{2T} for all $\Delta t \in [T, 2T)$, clearly all transitional fixed points must occur with $g^*_{\Delta t} \in [g_Q, \tilde{g}]$.

Now, recall from equation (7) that $A = (1, (1-I)/(E-1))$ is the unique point on the v-nullcline with $v = 1$. Thus, we have $g_Q > (1-I)/(E-1)$, while taking a backward flow implies that $\tilde{g} < (1-I)\exp(2\beta T)/(E-1)$. Therefore, $\tilde{g} - g_Q < (1-I)(\exp(2\beta T) - 1)/(E-1)$, which can be made small by taking E to be large or β to be small.

Consider next the value of g^*_{2T} for T large. As $T \to \infty$, $g^*_{2T} \to 2k$. Therefore, by taking $2k < (1-I)/(E-1)$, we guarantee that $g^*_T < g^*_{2T} < (1-I)/(E-1)$ and thus recruitment fails. Alternatively, if we now consider g^*_T for T small enough, we obtain the opposite conclusion. Namely, as $T \to 0$, $g^*_T \to \infty$, and since $g^*_{2T} > g^*_T$, this implies that for any $k > 0$, there exists a small enough T such that recruitment will occur. The large and small T results together imply that for any fixed $k < (1-I)/2(E-1)$, there exists an intermediate interval $[T_{lo}, T_{hi}]$ of T values for which $g^*_{2T} > \tilde{g}$, and the difference $g^*_{2T} - g^*_T = k(1-\exp(-\beta T))/(1-\exp(-2\beta T))$ can be made larger than $\tilde{g} - g_Q$ by choosing E large enough or β small enough. Thus for an interval of T values, we have both $g^*_{2T} > \tilde{g}$ and $g^*_T < g_Q$, implying that for this interval, synchronized input of size $2k$ that arrives with period $2T$ recruits, while input of period T and size k does not. □

The recruitment part of Lemma 3.12 establishes that under a few conditions on parameters, the intersection of $v^*_T(g)$ and g^*_T lies outside of ES. This intersection is a fixed point of the map P_T. Under these same conditions, the intersection of $v^*_{2T}(g)$ and g^*_{2T} lies inside ES or has $v > 1$, at a fixed point of the map P_{2T}. Since $P_{\Delta t}$ has a unique fixed point for each $\Delta t \in [T, 2T]$, there must be at least one Δt at which the corresponding fixed point lies in the boundary of ES. More specifically, by Lemmas 3.10 and 3.11, this fixed point must occur at Δt such that $\hat{R}_{\Delta t}$ is to the left of Q and must lie on $\hat{\Gamma}_{\Delta t} \subset \Gamma$. The natural question to ask at this point is whether or not this transitional fixed point is unique. By proving that it is, under certain conditions, we will now establish Theorems 3.13 and 3.15.

Theorem 3.13 *Fix parameters such that Lemma 3.12 holds, i.e. there exists an interval $[T_{lo}, T_{hi}]$ such that recruitment occurs for $\Delta t = 2T$ and fails for $\Delta t = T$ whenever*

$T \in [T_{lo}, T_{hi}]$. *For β sufficiently small, there exists $\Delta t_c \in (T, 2T)$ such that recruitment occurs if and only if $\Delta t > \Delta t_c$.*

Remark 3.14 Once parameters are fixed such that Lemma 3.12 holds, it will continue to hold if β is reduced.

Proof: Our goal is to show that there is exactly one value of $\Delta t \in (T, 2T)$ for which the fixed point $(v^*_{\Delta t}, g^*_{\Delta t})$ of $P_{\Delta t}$ lies in $\hat{\Gamma}_{\Delta t}$. Since the assumptions of non-recruitment for $\Delta t = T$ and recruitment for $\Delta t = 2T$ give the existence of at least one such Δt, it suffices to assume that $(v^*_{\Delta t}, g^*_{\Delta t})$ lies in $\hat{\Gamma}_{\Delta t}$ and show that if $\Delta t' < \Delta t$, then $(v^*_{\Delta t'}, g^*_{\Delta t'})$ cannot lie in $\hat{\Gamma}_{\Delta t'}$.

To argue by contradiction, suppose that $\Delta t' < \Delta t$ and that $(v^*_{\Delta t}, g^*_{\Delta t})$ and $(v^*_{\Delta t'}, g^*_{\Delta t'})$ lie in $\hat{\Gamma}_{\Delta t}$ and $\hat{\Gamma}_{\Delta t'}$, respectively. Note that both $\hat{\Gamma}_{\Delta t}$ and $\hat{\Gamma}_{\Delta t'}$ are contained within the same trajectory, Γ. Since $\Delta t' < \Delta t$, it follows from (16) that $g^*_{\Delta t'} < g^*_{\Delta t}$, meaning that $(v^*_{\Delta t'}, g^*_{\Delta t'})$ is closer to Q than is $(v^*_{\Delta t}, g^*_{\Delta t})$.

Let $(v_{\Delta t}(t), g_{\Delta t}(t))$, $(v_{\Delta t'}(t), g_{\Delta t'}(t))$ denote the trajectories emanating from the two initial conditions under consideration, We can calculate that $g_{\Delta t'}(\Delta t') > g_{\Delta t}(\Delta t)$, which implies that $v_{\Delta t'}(\Delta t') > v_{\Delta t}(\Delta t)$ and of course that $g_{\Delta t'}(\Delta t') + k > g_{\Delta t}(\Delta t) + k$. Hence, the trajectory generated by the flow from $(v_{\Delta t'}(t), g_{\Delta t'}(t) + k)$ is bounded between the trajectory generated by the flow from $(v_{\Delta t}(t), g_{\Delta t}(t) + k)$ and Γ itself. Further, note that the trajectory from $(v_{\Delta t'}(t), g_{\Delta t'}(t) + k)$ must satisfy

$$g_{\Delta t'}(2T) = g_{\Delta t'}(0) - k < g_{\Delta t}(0) - k = g_{\Delta t}(2T). \tag{20}$$

We can now prove that the theorem holds for β sufficiently small. By making β sufficiently small, we can assume that trajectories that reach the v-nullcline follow it arbitrarily closely. In this case, $(v_{\Delta t}(2T), g_{\Delta t}(2T))$ and $(v_{\Delta t'}(2T), g_{\Delta t'}(2T))$ both lie as close as we wish to the v-nullcline. Hence, condition (20) implies that $v_{\Delta t'}(2T) < v_{\Delta t}(2T)$. But then the fixed point conditions $v_{\Delta t'}(0) = v_{\Delta t'}(2T)$ and $v_{\Delta t}(0) = v_{\Delta t}(2T)$ imply $v_{\Delta t'}(0) < v_{\Delta t}(0)$, which contradicts the fact that $\Delta t' < \Delta t$ with $(v_{\Delta t}(0), g_{\Delta t}(0)), (v_{\Delta t'}(0), g_{\Delta t'}(0))$ both on Γ. □

A schematic illustration of a trajectory corresponding to a fixed point on Γ for β small is given in Figure 9. Note that trajectories from different initial conditions on Γ will be strongly compressed in their v-coordinates, as used in the proof of Theorem 3.13.

The following theorem presents a second rigorous result on the transition from non-recruitment to recruitment, corresponding to the case when T is small. This result is weaker than the case of small β, in that it does not rule out multiple transitions before the final transition to recruitment occurs, but it does rule out the possibility that there

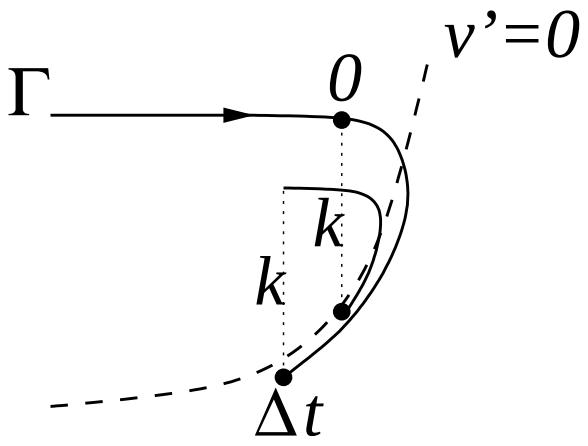

Figure 9: Schematic illustration of a trajectory corresponding to a fixed point on Γ for β small. The initial condition is labeled 0 and the location of the trajectory at the first input time is labeled Δt.

are transitions arbitrarily close to $\Delta t = 2T$ and it also gives a precise bound on how small T has to be.

Theorem 3.15 *Fix T sufficiently small such that*

$$g_Q < \frac{k}{1 - e^{-2\beta T}},$$

where g_Q depends on $k, \beta, E,$ and I but not on T. If, for this T, recruitment fails for $\Delta t = T$ and succeeds for $\Delta t = 2T$, then there exists a unique value $\Delta t_c \in (T, 2T)$ such that recruitment occurs for all $\Delta t \in (\Delta t_c, 2T]$.

Proof: Let $\hat{R}_{\Delta t}$ be denoted by $(\hat{v}_{\Delta t}, \hat{g}_{\Delta t})$. If recruitment fails for $\Delta t = T$ but not for $\Delta t = 2T$, then there exists a value $\Delta t_f \geq T$ such that recruitment fails for $\Delta t \in [T, \Delta t_f]$ and such that $g^*_{\Delta t_f} < \hat{g}_{\Delta t_f}$, by Lemma 3.11. To establish the theorem, we will first show that for T sufficiently small, $g^*_{2T} > \hat{g}_{2T}$, which implies that the curves $g^*_{\Delta t}$ and $\hat{g}_{\Delta t}$ intersect for some $\Delta t \in (\Delta t_f, 2T)$, and $dg^*_{\Delta t}/d(\Delta t) > d\hat{g}_{\Delta t}/d(\Delta t)$ for all $\Delta t \in [T, 2T]$, which implies that this intersection is unique.

Equation (16) gives the formula for $g^*_{\Delta t}$. In Appendix C, we derive the expression $\hat{g}_{\Delta t} = g_Q e^{\beta \Delta t}(1 - k/g_Q)$, where $g_Q > k$ satisfies equation (28) and therefore depends on $k, \beta, E,$ and I but not on T. ¿From these equations, we find that both quantities have positive derivatives with respect to Δt and that $dg^*_{\Delta t}/d(\Delta t) > d\hat{g}_{\Delta t}/d(\Delta t)$ for all $\Delta t \in [T, 2T]$ if and only if

$$g_Q < k/(1 - \exp(-2\beta T)), \tag{21}$$

which is true for T sufficiently small with all other parameters fixed. Similarly, after some algebraic manipulation, $g^*_{2T} > \hat{g}_{2T}$ if and only if

$$g_Q < k(\exp(2\beta T) + 1)/(\exp(2\beta T) - 1), \tag{22}$$

which also holds for T sufficiently small and all else fixed. In fact, since $(\exp(2\beta T) + 1)/(\exp(2\beta T) - 1) > 1/(1 - \exp(-2\beta T))$, the condition given by (22) is redundant. Thus, for any T such that equation (21) holds, the curves $g^*_{\Delta t}$ and $\hat{g}_{\Delta t}$ intersect uniquely on $(\Delta t_f, 2T)$, and we call the intersection value $\Delta t = \Delta t_c$.

Now, to conclude the proof of the theorem, it suffices to show that recruitment occurs for all $\Delta t > \Delta t_c$. This holds because $g^*_{\Delta t} > \hat{g}_{\Delta t}$ for all $\Delta t > \Delta t_c$, and hence the fixed point of $P_{\Delta t}$ must lie outside of $\hat{\Gamma}_{\Delta t}$ for all $\Delta t > \Delta t_c$, by Lemma 3.11. Thus, there cannot be any transitions between recruitment and non-recruitment for $\Delta t > \Delta t_c$, and since recruitment occurs for $\Delta t = 2T$, it must also occur for all $\Delta t \in (\Delta t_c, 2T]$. □

3.3 Theta model - single input

Consider the theta neuron with periodic excitatory input, given by the equations (6) and (4). As with the IF neuron, we start by asking whether the input will recruit the model neuron to fire, or cross through $\theta = \pi$, repetitively, as defined in Section 3.1. Again, we will define a two-dimensional map, in this case based on the flow of (6). We shall see that for the theta model, recruitment is determined by the existence or non-existence of a fixed point of this map, rather than by the location of a fixed point that always exists, as in the IF case. Our result that recruitment will occur if and only if a certain fixed point of this map exists will be made precise at the end of this subsection, in Theorem 3.19.

Now, since $g' = -\beta g$ between inputs, which are each of size k, equation (8), namely

$$g^* = \frac{k}{1 - e^{-\beta T}},$$

again gives the unique value of g such that if $g(0^+) = g^*$, then $g(T^+) = g^*$. Similarly, for fixed g, we can ask whether there exists one or more values $\theta^*(g)$ such that, under the flow of system (6) with $\theta(0) = \theta^*(g)$, the condition $\theta(T) = \theta^*(g)$ holds. First, recall that the critical points of (6) are the points $(\theta_S, 0), (\theta_U, 0)$ with $\theta_S < 0 < \theta_U$. Note that the θ-nullcline partitions the $\{g \geq 0\}$ part of the phase plane for system (6) into two regions, with $\theta' < 0$ below the θ-nullcline, and $\theta' > 0$ above it. Denote the left branch of the θ nullcline by $\Theta_- = \{(\theta_-(g), g)\}$ and the right branch by $\Theta_+ = \{(\theta_+(g), g)\}$. Let B denote the region bounded above by the θ-nullcline and below by $\{g = 0\}$, as shown in Figure 10. The following preliminary result will be useful as we proceed.

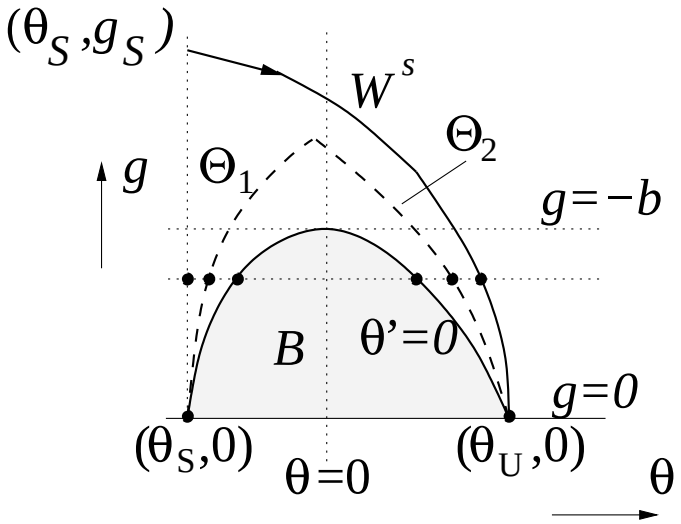

Figure 10: Basic picture for the derivation of the curves $\Theta_1 = (\theta_1(g), g), \Theta_2 = (\theta_2(g), g)$, where $\Delta\theta = 0$. The shaded region B is bounded above by the θ-nullcline, which consists of $\Theta_- \cup \Theta_+$ and is simply labelled by $\theta' = 0$ here. On the first horizontal dotted curve above $g = 0$, six points are marked. Moving from largest θ to smallest θ, these are: a point on W^s, with $\Delta\theta > 0$; a point on Θ_2, with $\Delta\theta = 0$; a point on Θ_+, with $\Delta\theta < 0$ by Lemma 3.16; a point on Θ_-, with $\Delta\theta < 0$ by Lemma 3.16; a point on Θ_1, with $\Delta\theta = 0$; and a point on $\theta = \theta_S$, with $\Delta\theta > 0$ by Lemma 3.16. Note that Θ_1, Θ_2 need not coalesce precisely as shown, as discussed below Lemma 3.18, and that $\Theta_1 \cup \Theta_2$ are bounded by W^s and $\{\theta = \theta_S\}$, as in Theorem 3.19ii.

Lemma 3.16 *If $(\theta(t), g(t))$ is a solution to system (6) with $(\theta(0), g(0))$ on the θ-nullcline, then $\theta(t) < \theta(0)$ for all $t > 0$.*

Proof: The θ-nullcline exists for $g < -b$, where $b < 0$ appears in (6). The vector field along the θ-nullcline points into B since $d\theta_+(g)/dg < 0$ and $d\theta_-(g)/dg > 0$, and $g' < 0$ for $g > 0$. Therefore B is positively invariant. Also if $(\theta(0), g(0)) \in B$, then $\theta'(t) < 0$ for each $t > 0$, which yields $\theta(t) < \theta(0)$ for all $t > 0$. □

Let $\Delta\theta = \theta(T) - \theta(0)$ for any initial condition $(\theta(0), g(0))$; we omit explicit reference to the dependence of $\Delta\theta$ and $\theta(T)$ on $g(0)$ and on $\theta(0)$. We now begin to characterize the set of points where $\Delta\theta = 0$, as illustrated in Figure 10.

Lemma 3.17 *There exist $g^c \geq g_c > -b > 0$ such that:*

i) For each $g \in [0, g_c)$, there are at least two values, $\theta_1(g) < \theta_2(g)$, such that, if

$(\theta(0), g(0)) = (\theta_i(g), g)$ *for* $i = 1$ *or* 2*, then under the flow of system (6),* $\theta(T) = \theta(0)$.

ii) The functions $\theta_1(g), \theta_2(g)$ *satisfy*

$$\theta_1(g) \to \theta_S \text{ and } \theta_2(g) \to \theta_U \text{ as } g \downarrow 0. \tag{23}$$

iii) If $g > g^c$*, then* $\theta(T) > \theta(0)$ *for all initial conditions* $(\theta(0), g)$.

Proof: Denote the $\{g > 0\}$ branch of the stable manifold of the saddle point $(\theta_U, 0)$ by $W^s = \{(\theta^s(g), g) : g > 0\}$. Note that along this manifold, $\theta' > 0$. Now consider $\Delta\theta$ for various choices of $(\theta(0), g(0))$. Since W^s is invariant, if $(\theta(0), g(0)) \in W^s$, then $\Delta\theta > 0$. Further, for fixed $g < -b$, where the θ-nullcline exists, and $(\theta(0), g(0)) \in \Theta_+$, Lemma 3.16 implies that $\Delta\theta < 0$. Thus, by the intermediate value theorem, there exists $\theta_2(g) \in (\theta_+(g), \theta^s(g))$ such that $\Delta\theta = 0$ for $\theta(0) = \theta_2(g)$. Moreover, since $\theta^s(g) \to \theta_+(0) = \theta_U$ as $g \downarrow 0$, the squeeze lemma implies the second limit in equation (23).

Similarly, $\Delta\theta < 0$ for $(\theta(0), g(0)) \in \Theta_-$, by Lemma 3.16. Further, if $\theta(0) < \theta_S$, the θ-coordinate of the stable critical point of (6), then $\Delta\theta > 0$, again using Lemma 3.16 to note that $\theta(T) > \theta_S > \theta(0)$ if $(\theta(t), g(t))$ enters B. Hence, there exists $\theta_1(g) \in (\theta_S, \theta_-(g))$ such that $\Delta\theta = 0$ for $\theta(0) = \theta_1(g)$, with the first limit in equation (23) following from the facts that $\theta_-(g) \to \theta_S$ as $g \downarrow 0$ and that $\Delta\theta > 0$ for all initial conditions $(\theta(0), 0)$ with $\theta(0) < \theta_S$.

By continuity in initial conditions, the curves $\Theta_1 = (\theta_1(g), g), \Theta_2 = (\theta_2(g), g)$ extend to $g > -b$, at least for g sufficiently close to $-b$. On the other hand, if g is sufficiently large, then for each $(\theta(0), g(0))$, we have $g(T) > -b$. Thus, the trajectory from $(\theta(0), g(0))$ remains above the θ-nullcline, with $\theta' > 0$, for all $t \in [0, T]$, and $\Delta\theta > 0$ results. This establishes the desired conclusion. □

The reason that we distinguish g^c from g_c in Lemma 3.17 is that in theory, the curves $\Theta_i = (\theta_i(g), g)$ could undergo various bifurcations, giving rise to additional branches satisfying $\Delta\theta = 0$, for some range of $g < g^c$. We next provide some constraints on the set $\Theta \doteq \{(\theta, g) : \Delta\theta = 0\}$; again, see Figure 10.

Lemma 3.18 *For* $g \leq -b$*, the curves* Θ_1, Θ_2 *contain the only sets of initial conditions for which* $\Delta\theta = 0$*; that is,* $\Theta \cap \{(\theta, g) : 0 \leq g \leq -b\} \subset \Theta_1 \cup \Theta_2$*. Moreover,* $\Theta \cap \{(\theta, g) : \theta > 0, g < 1 - b\} \subset \Theta_2$*. Finally,* $d\theta_2(g)/dg \leq 0$ *and* $d\theta_1(g)/dg \geq 0$ *on any intervals* $(0, g)$ *of* g*-values on which they exist, and at any fixed* $\tilde{\theta}$*, the sets* $\Theta_1 \cap \{\theta = \tilde{\theta}\}$ *and* $\Theta_2 \cap \{\theta = \tilde{\theta}\}$ *are either unique points or are empty.*

Proof: From system (6), note that

$$\frac{d}{d\theta}\left(\frac{d\theta}{dt}\right) = (1 - b - g)\sin\theta. \tag{24}$$

Hence, if $g < 1 - b$, then $d(\theta')/d\theta > 0$ for $\theta \in (0, \pi)$, including the region between Θ_+ and W^s, and $d(\theta')/d\theta < 0$ for $\theta \in (-\pi, 0)$, including the region to the left of Θ_-.

Now, suppose that for some $(\theta(0), g(0))$ with $\theta(0) > 0$ and $g(0) < 1 - b$, we have $\Delta\theta = 0$. This is equivalent to the condition

$$\int_0^T \theta'(t)\, dt = 0. \tag{25}$$

Note that the trajectory from $(\theta(0), g(0))$ satisfies $\theta(t) \geq \theta(0) > 0$ for all $t \in [0, T]$. Hence, if we consider any $\tilde{\theta}(0) > \theta(0)$, then $\tilde{\theta}(t) > \theta(t)$ for all $t \in [0, T]$ and thus $\tilde{\theta}'(t) > \theta'(t)$ for all $t \in [0, T]$, and equation (25) cannot hold for the new trajectory; see Figure 11. Similarly, if $0 < \tilde{\theta}(0) < \theta(0)$, then $\tilde{\theta}'(t) < \theta'(t)$ for all $t \in [0, T]$ for which $\tilde{\theta}(t) > 0$. If $\tilde{\theta}(t) > 0$ on all of $[0, T]$, then equation (25) again cannot hold, whereas if $\tilde{\theta}(t_0) = 0$ for some $t_0 \in (0, T)$, then $\tilde{\theta}(t_0)$ lies inside B, beneath the θ-nullcline. Thus, $\tilde{\theta}(t) < \tilde{\theta}(t_0) = 0 < \tilde{\theta}(0)$ for all $t \in (t_0, T]$, and $\Delta\theta < 0$ results. This establishes that $\Theta \cap \{(\theta, g) : \theta > 0, g < 1 - b\} \subset \Theta_2$ (see Figure 11A). The argument implying that $\Theta \cap \{(\theta, g) : \theta < 0, g \leq -b\} \subset \Theta_1$ is analogous, since trajectories with initial conditions $(\theta(0), g(0))$ satisfying $\theta(0) < \theta_-(g(0)), g(0) \leq -b$ cannot cross $\{\theta = 0\}$ by Lemma 3.16. However, it does not extend to $g \in (-b, 1 - b)$ because for $g(0) > -b$, it is possible that some trajectory could cross through $\{\theta = 0\}$ and achieve $\Delta\theta = 0$.

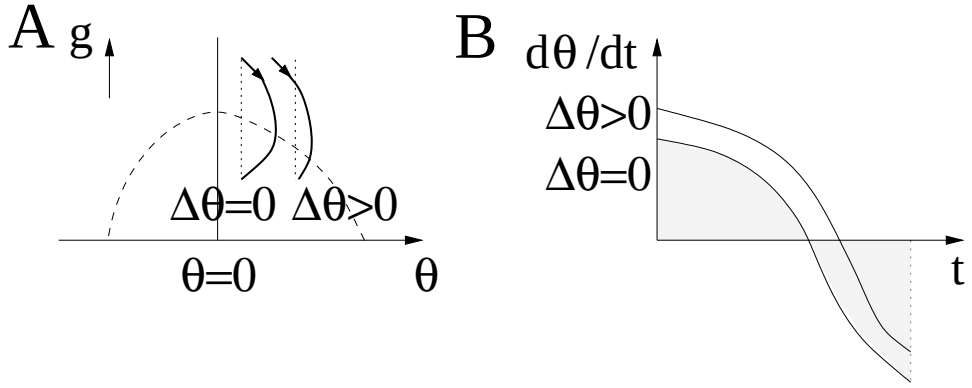

Figure 11: Argument for the uniqueness of Θ_2 in $\{(\theta, g) : \theta > 0, g < 1 - b\}$. A) Given an initial condition in this set for which $\Delta\theta = 0$, any initial condition with the same g value and larger θ yields $\Delta\theta > 0$; an example is shown in the (θ, g) plane. B) The same result, illustrated using time courses of $d\theta/dt$. For the time course that gives $\Delta\theta = 0$, the two shaded areas are equal, as stated in equation (25). Since $d\theta/dt$ is larger everywhere on the other time course, by equation (24), $\Delta\theta > 0$ results.

Next, we prove that $d\theta_2(g)/dg \leq 0$ and that there cannot exist two different g values

sharing the same $\theta_2(g)$. Suppose that $(\theta(0), g(0))$ lies on the curve Θ_2, and label the corresponding trajectory $(\theta(t), g(t))$. Consider also $(\theta(0), \tilde{g}(0))$ with $\tilde{g}(0) > g(0)$, and label the corresponding trajectory $(\tilde{\theta}(t), \tilde{g}(t))$. If $g(t_1) = \tilde{g}(t_2)$, then by uniqueness of solutions of (6), $\tilde{\theta}(t_2) > \theta(t_1)$, while by the exponential decay of g, $t_2 > t_1$. Since $\theta(t) \geq \theta(0)$ on $[0, T]$, it follows that $\tilde{\theta}(t) > \theta(0)$ on $[0, T]$, and therefore $\theta_2(\tilde{g}) \neq \theta_2(g)$. Thus, two different g values cannot share the same $\theta_2(g)$ and also $d\theta_2(g)/dg$ cannot change signs, and it remains to determine whether it is nonpositive or nonnegative. To do this, suppose that in the above argument, g is selected such that $\theta_2(g) > 0$. The above argument gives $\Delta\theta > 0$ for any initial condition $(\theta_2(g), \tilde{g})$ with $\tilde{g} > g$. Comparing any trajectory emanating from $(\tilde{\theta}, \tilde{g})$, with $\tilde{\theta} > \theta_2(g)$, to the trajectory from $(\theta_2(g), \tilde{g})$ shows that again $\Delta\theta > 0$, again by uniqueness and equation (24). Hence, $\theta_2(\tilde{g}) < \theta_2(g)$ for $\tilde{g} > g$. Thus, $d\theta_2(g)/dg < 0$ at least for $g < -b$, where $\theta_2(g) > 0$, and hence $d\theta_2(g)/dg \leq 0$ for all g for which it is defined, as claimed.

Finally, the proofs that $d\theta_1(g)/dg \geq 0$ and that no two g values share the same $\theta_1(g)$ are similar, where we can establish the sign of $\theta_1'(g)$ by using g sufficiently small such that the trajectory from $(\theta_1(g), g)$ remains in $\{\theta < 0\}$. □

Next, we consider how the curves Θ_i terminate as g increases, which clearly must occur, as stated in Lemma 3.17, since they are bounded by W^s. By Lemma 3.18, each curve Θ_i cannot undergo a pitchfork bifurcation, a transcritical bifurcation, or a saddle-node bifurcation in which $d\theta_i(g)/dg = 0$, since each of these requires the existence of two points (θ, g_1), (θ, g_2) with $g_1 \neq g_2$ that both yield $\Delta\theta = 0$, which contradicts the proof of Lemma 3.18.

One possibility that remains is that Θ_1 and Θ_2 meet and terminate at some value of g, corresponding to a saddle-node bifurcation in the set of fixed points of the θ component of map Π, if g is considered as a bifurcation parameter. The only other remaining possibility is that, as g increases, Θ_1 and Θ_2 terminate in separate saddle-node bifurcations with other, intermediate, curves along which $\Delta\theta = 0$; see Figure 12. But since the Θ_i are the unique such curves for $g < -b$, these other curves must have a lower bounds $\underline{g}_1, \underline{g}_2 > -b$, and an additional saddle-node bifurcation must occur at each of these bounds. Applying this argument repeatedly, the curves Θ_1, Θ_2 would, at their respective terminations, be linked by a snaking curve, composed of alternating negatively and positively sloped segments, corresponding to a finite sequence of one or more saddle-node bifurcations, with finiteness ensured by the fact that all of the bifurcations would occur on a bounded interval of θ values and that the vector field of (6) is analytic, which rules out accumulations of bifurcation points. Figure 13 shows a numerical example in which the set Θ consists simply of the union of the two curves Θ_1, Θ_2, which coalesce in a single saddle-node bifurcation.

Given this rather complete characterization of the set of points, Θ, at which $\Delta\theta = 0$,

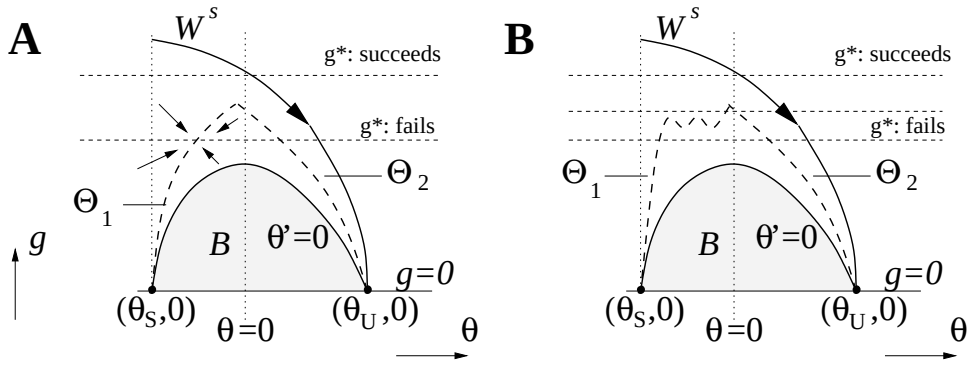

Figure 12: Possible scenarios for fixed points of Π. Dashed curves correspond to Θ, where $\Delta\theta = 0$, and $g = g^*$, where $\Delta g = 0$; in each panel, multiple possible positions of $g = g^*$ are shown. A) Here, Θ consists only of $\Theta_1 \cup \Theta_2$. If g^* is sufficiently high to avoid fixed points, then recruitment succeeds, while if it is low enough, then an attracting fixed point of Π exists on Θ_1 and recruitment fails. Arrows show the directions of change in θ, g, upon application of Π, in a neighborhood of the attracting fixed point for the latter choice of g^*. B) Here, Θ_1 and Θ_2 are joined by a sequence of saddle-node bifurcations. Again, recruitment succeeds for large g^*. As long as there exists an attracting fixed point of Π, which may or may not be on Θ_1, recruitment fails, as indicated by two of the g^* locations shown.

we now consider the map $\Pi(\theta, g)$ defined by the flow of system (6) for time T, followed by an input of size k that resets g as described in equation (4). Fixed points of Π can only occur at the g value g^* given in equation (8). Recruitment will be determined by the nature of the set of fixed points of Π. Recall that for the theta model, firing occurs at $\theta = \pi$. This arises if and only if an input resets a point across W^s, since $\{\theta = \pi\}$ lies to the right of W^s, trajectories cannot cross W^s under the flow of (6) without reset, and the region to the right of W^s is invariant under Π.

Now, if g^* is sufficiently large, corresponding to large k or small βT, then Π has no fixed points. In this case, all initial conditions are recruited. To see this, note that the curve $\{g = g^*\}$ is invariant and attracting under Π, since $g(0) < g^*$ ($g(0) > g^*$) yields $g(T) + k > g(0)$ ($g(T) + k < g(0)$). But if $\{g = g^*\}$ lies in the region where $\Delta\theta > 0$ for all initial θ, then all points will get mapped across W^s under repeated iteration of Π.

Alternatively, suppose that g^* is sufficiently small that Π has two or more fixed points, corresponding to small k or large βT. Consider the fixed point of Π with minimal θ value, call it $(\theta_m^*, g^*) \in \Theta_1$. Note that $\Theta = \{(\theta, g) : \Delta\theta = 0\}$ separates the (θ, g) plane into two regions, such that above Θ, $\Delta\theta > 0$, while below Θ, $\Delta\theta < 0$. The point

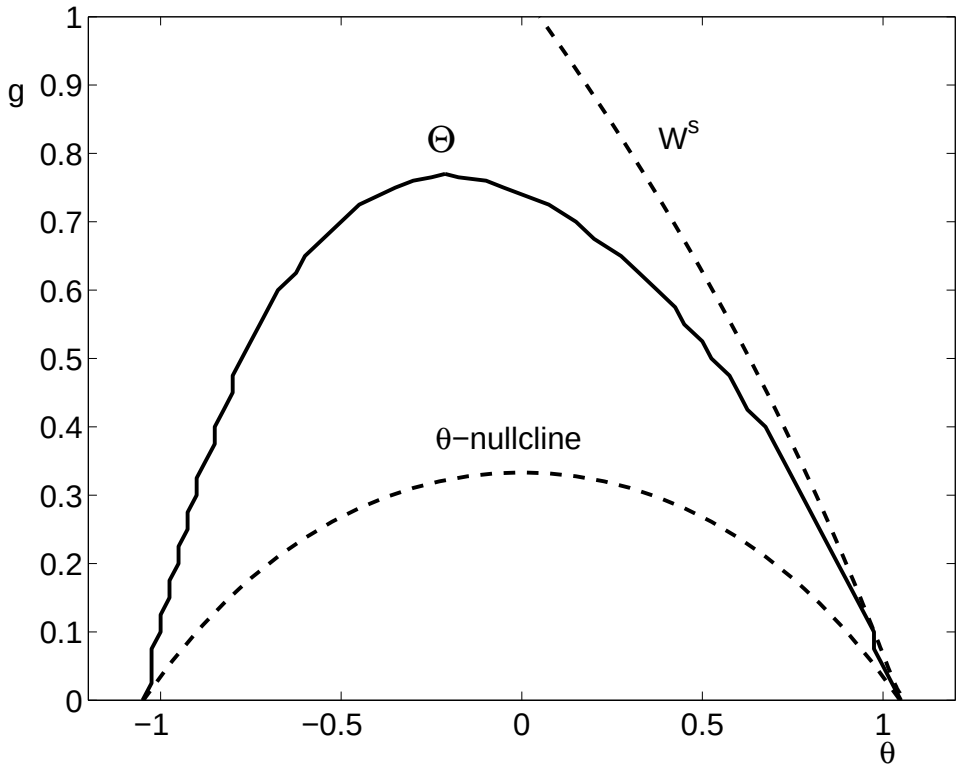

Figure 13: An example of the set Θ where $\Delta\theta = 0$, along with the stable manifold W^s and the θ-nullcline (dashed). All curves were generated numerically from equations (5),(3) with $b = -1/3, \beta = 1$, and integration time $T = 2$.

$(\theta_m^*, g^*) \in \Theta$ necessarily lies on a branch of Θ with positive slope, such that we cross from the $\Delta\theta > 0$ region to the $\Delta\theta < 0$ region as we increase $\theta(0)$ through θ_m^* with $g = g^*$; see Figure 12. The fixed point (θ_m^*, g^*) is therefore attracting for Π, and hence recruitment fails in this case; that is, after at most a finite number of firings, every cell will enter the basin of attraction of (θ_m^*, g^*), or of another attracting fixed point if multiple saddle-node bifurcations along Θ exist, and fall silent.

Finally, if we treat g^* as a bifurcation parameter and increase it without affecting the location of Θ, as may be done by increasing k, then it will pass through the values at which all of the finitely many saddle-node bifurcations in Θ occur. Let $\bar{g}_b$ denote the maximum of these values. We can now rigorously establish the following intuitively sensible theorem; also see Figure 12.

Theorem 3.19 *i) If k, β, T in system (6) with reset condition (4) are chosen such that $g^* < \bar{g}_b$, then the map Π has an attracting fixed point and recruitment fails for all initial conditions in the set $\{(\theta, g) : \theta \in [-\pi, \pi], g \geq 0\}$. If $g^* > \bar{g}_b$, then Π has no fixed points and all initial conditions in this set are recruited.*

ii) Let $(\theta_S, g_S) = W^s \cap \{\theta = \theta_S\}$ (see Figure 10). If $\Theta_2 \cap \{\theta = 0\}$ exists, then $\bar{g}_b \in (g_0, g_S)$, where $(0, g_0) = \Theta_2 \cap \{\theta = 0\}$. Otherwise, $\bar{g}_b \in (1 - b, g_S)$.

iii) Recruitment occurs if k is made sufficiently large or if β or T is made sufficiently small. Recruitment fails if β or T is made sufficiently large and k is not too large.

Proof: Part i) has been established. For part ii), the lower bounds on $\bar{g}_b$ follow from Lemma 3.18. The upper bound on $\bar{g}_b$ holds because Θ_1, Θ_2 must lie between $\{\theta = \theta_S\}$ and W^s, so they must coalesce within the region bounded by these curves.

In iii), the dependence of recruitment on k follows immediately from the effect of k on g^*, given in equation (8). The effects of β and T are more subtle, since the set Θ depends on β, T as well. The result for T holds because as T is decreased, $g^* \to \infty$, but Θ remains bounded by W^s, so recruitment eventually occurs. On the other hand, as T is increased, $g^* \downarrow k$, by equation (8). At the same time, for fixed g, the set Θ expands, with its left boundary Θ_1 moving to smaller θ and its right boundary Θ_2 moving to larger θ; these changes both favor the existence of fixed points. To see the effect of T on Θ, consider an initial condition $(\theta(0), g(0)) \in \Theta_2$ for fixed $T = T_1$, with corresponding trajectory $(\theta(t), g(t))$ for $t \in [0, T]$. For times near T, $\theta'(t) < 0$. For $T = T_2 > T_1$, the trajectory from (θ, g) follows $(\theta(t), g(t))$ up to time T_1 and then continues, with $\theta'(t) < 0$ for $t \in [T_1, T_2]$. Hence, $\Delta\theta < 0$ for this initial condition with $T = T_2$, and $\theta_2(g) > \theta(0)$ for $T = T_2$. A similar argument proves that $\theta_1(g)$ moves to more negative θ values as T increases. These changes allow Θ to cross $\{g = k\}$ if k is not too large (e.g. if $k < -b$, although clearly this can be sharpened).

The proof of the result for β is analogous to that for T. Note that β and T appear in a product in equation (8), so β has an identical effect to T there. Finally, as with T, increases in β lead to an expansion of Θ, which complements the decrease in g^* to promote formation of fixed points. For example, suppose that $(\theta(0), g(0)) \in \Theta_2$ with $\beta = \beta_1$ and then consider $\beta = \beta_2 > \beta_1$. Faster decay of g leads to less positive (or more negative) $d\theta/dt$, by equation (5), and hence $\Delta\theta < 0$ results, such that Θ_2 must move to larger θ values. The proof that Θ_1 moves to smaller θ as β increases is similar. □

3.4 Theta model - 2 inputs

3.4.1 Definitions and parameter selection

As we did for the IF model, we now wish to consider pairs of periodic inputs of size k, one of which arrives at times $0, 2T, 4T, \ldots$ and the other of which arrives at times $\Delta t, 2T + \Delta t, 4T + \Delta t, \ldots$, with $T \leq \Delta t \leq 2T$. For given Δt, we define a map, $\Pi_{\Delta t}(\theta, g)$, by flowing the initial condition $(\theta(0), g(0))$ under equation (6) for time Δt, applying the reset condition $g(\Delta t^+) = g(\Delta t^-) + k$, flowing for an additional time $2T - \Delta t$ after reset, and resetting again. In analogy with the single input case, we seek to determine whether or not recruitment occurs by studying the set of fixed points of $\Pi_{\Delta t}$. Similarly to the IF case, the set of fixed points can be viewed as the intersection of curves $g^*_{\Delta t}$, for which $g(2T^+) = g(0^+)$, and $\theta^*_{\Delta t}$, for which $\theta(2T^+) = \theta(0^+)$. Further, since the g dynamics decouple from the θ dynamics in (6), $g^*_{\Delta t}$ is again given by equation (16). The challenge that remains is to characterize $\theta^*_{\Delta t}$, which is the generalization of the set Θ from the single-input case.

To start, note that the value of k is irrelevant for defining θ^*_{2T}, since when $\Delta t = 2T$, a single input arrives with period $2T$ and there is no reset during time $(0, 2T)$. Thus, Lemmas 3.17, 3.18 imply the existence of the set θ^*_{2T}, consisting of curves Θ_1 and Θ_2, connected by one or more saddle-node bifurcations. For $\Delta t \in (T, 2T)$, $\Pi_{\Delta t}$ features a reset of size k during $(T, 2T)$, and this greatly impacts the location of $\theta^*_{\Delta t}$. In particular, suppose that k is quite large, with $k \gg -b$. Then after reset, $\theta' > 0$, no matter what the value of θ was before reset. This means that if k is sufficiently large, $\theta^*_{\Delta t}$ may fail to exist at all, except for Δt values extremely close to $2T$. In such a case, however, clearly there is recruitment for all Δt, so this is not interesting to analyze. We shall henceforth restrict our discussion to parameter regimes for which $\theta^*_{\Delta t}$ exists for all $\Delta t \in [T, 2T]$. In such regimes, we have the following lemma.

Lemma 3.20 *Fix any $\Delta t \in [T, 2T]$ and denote each constant-g section of $\theta^*_{\Delta t}$ by $\theta^*_{\Delta t}(g)$, although this may contain more than one point. If $k < -b$, then there exists $g_0 > 0$ such that $\theta^*_{\Delta t}(g)$ consists of exactly two points for each $g \in [0, g_0)$. The results holds, for example, for $g_0 = (-b - k)e^{\beta \Delta t}$.*

Proof: First, consider $(\theta(2T), g(2T))$, generated by applying the map $\Pi_{\Delta t}$ to various $(\theta(0), g)$ for fixed g. Note that $\theta(2T) > \theta(0)$ for $\theta(0) = \theta_S$, while $\theta(2T) > \theta(0)$ as well for $\theta(0) = \theta^s(g)$ defined such that $(\theta^s(g), g) \in W^s$. Moreover, for $\theta(0) = 0$, we have $\theta(\Delta t^-) < \theta(0)$, since $(\theta(0), g)$ lies in B, beneath the θ-nullcline. Further, if $g < (-b - k)e^{\beta \Delta t}$, then $g(\Delta t^+) < -b$ and $\theta(\Delta t^+) \equiv \theta(\Delta t^-) < \theta(0) = 0$ ensure that $\theta(2T) < \theta(\Delta t)$. Hence, by the intermediate value theorem, there are at least two elements in $\theta^*_{\Delta t}$ for this g, call them $(\theta_1(g), g), (\theta_2(g), g)$ with $\theta_1(g) < 0 < \theta_2(g)$. Further, the trajectory from $(\theta_1(g), g)$ stays in the region $\{\theta < 0\}$ over the full $2T$ period with reset, while $\theta_2(g) > 0$.

Now, note that equation (24) holds here, in between resets. Thus, there can be at most one $(\theta, g) \in \theta^*_{\Delta t}(g)$ such that the trajectory from (θ, g) stays in the region $\{\theta < 0\}$ over the full $2T$ period with reset. Similarly, there can be at most one $(\theta, g) \in \theta^*_{\Delta t}(g)$ for which $\theta > 0$. This completes the proof. □

To proceed further, it is important to note that, in theory, there are two different candidates for the curve to which $\theta^*_{\Delta t}$ converges as $\Delta t \downarrow T$, analogously to the IF case. Similarly to what was done there, we use the notation θ^*_T to define the curve where $\theta(T^+) = \theta(0^+)$, for which k is again irrelevant. As $\Delta t \downarrow T$, $\theta^*_{\Delta t}$ in fact converges not to θ^*_T but rather to a curve that we denote $\theta^*_{T\cup T}$, for which $\theta(2T^+) = \theta(0^+)$, with a reset of size k at time T. While θ^*_T differs from $\theta^*_{T\cup T}$, they must intersect at $g = g^*_T$. In fact, using $\theta^*_T(g)$ and $\theta^*_{T\cup T}(g)$ to denote the points in θ^*_T and $\theta^*_{T\cup T}$, respectively, with a given g-coordinate, we have the following result, which parallels the IF 2-input case.

Lemma 3.21 *Fix all parameters and assume that g is fixed such that $\theta^*_T(g), \theta^*_{T\cup T}(g)$ both exist. If $g < g^*_T$, then $\min_\theta\{(\theta, g) \in \theta^*_T(g)\} < \min_\theta\{(\theta, g) \in \theta^*_{T\cup T}(g)\}$, while $\max_\theta\{(\theta, g) \in \theta^*_T(g)\} > \max_\theta\{(\theta, g) \in \theta^*_{T\cup T}(g)\}$. If $g > g_{T*}$, then these relations are reversed, and finally $\theta^*_T(g^*_T) = \theta^*_{T\cup T}(g^*_T)$; see Figure 14.*

Proof: Suppose that $g < g^*_T$. For any trajectory $(\theta(t), g(t))$ defined for $t \in [0, 2T]$, with a reset $g(T^+) = g(T^-) + k$ at time T, it follows that

$$g(T^+) > g(T^-). \tag{26}$$

Choose $(\theta(0), g(0)) \in \theta^*_T$ such that $g(0) = g$ and $\theta(0) = \min_\theta\{(\theta, g) \in \theta^*_T(g)\}$. This choice yields $\theta(T) = \theta(0)$. But since equation (26) holds, the segment $\{(\theta(t), g(t)) : t > T\}$ is forced to the right of the segment $\{(\theta(t), g(t)) : t < T\}$, by uniqueness of solutions of equations (5),(3), and furthermore, $g(2T) > g(T)$. Thus, $\theta(2T) > \theta(0)$, as illustrated in Figure 14, so the minimal-θ element $(\theta, g) \in \theta^*_{T\cup T}(g)$ lies to the right of $(\theta(0), g)$. Similar consideration of $\theta(0) = \max_\theta\{(\theta, g) \in \theta^*_T(g)\}$ yields $\theta(2T) > \theta(0)$, so the maximal-θ element in $\theta^*_{T\cup T}(g)$ lies to the left of $(\theta(0), g)$. Finally, reset and uniqueness give the desired results for $g > g^*_T$ in the same way; see Figure 14. □

Since θ^*_T and $\theta^*_{T\cup T}$ intersect at $g = g^*_T$, the maps $\Pi_T, \Pi_{T\cup T}$ share the same fixed points, and either can be used to study recruitment for $\Delta t = T$. Taking advantage of this observation, we next show that it is possible to select parameters such that Π_{2T} has no fixed points, and thus recruitment occurs for $\Delta t = 2T$, while Π_T has an attracting fixed point, and thus recruitment fails for $\Delta t = T$. Recall that the maximum point of the θ-nullcline lies at $(\theta, g) = (0, -b)$, where $b < 0$, that $(\theta_S, 0)$ is the stable critical point of (6), that W^s is the stable manifold of the saddle point $(\theta_U, 0)$ of (6), and that we use (θ_S, g_S) to denote $W^s \cap \{\theta = \theta_S\}$.

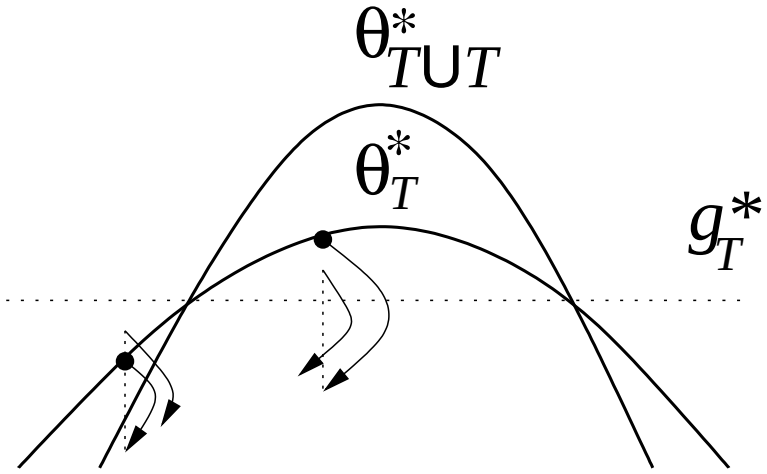

Figure 14: The relative positions of θ_T^* and $\theta_{T\cup T}^*$. If a point on θ_T^* is evolved, then $\theta(T) = \theta(0)$ results. After reset (dotted vertical lines), the continuing trajectory on $(T, 2T]$ is bounded by that produced on $[0, T]$. If the initial g is below g_T^*, then $\Delta\theta > 0$ necessarily ensues, while if the initial g is above g_T^*, then $\Delta\theta < 0$ follows.

Lemma 3.22 *Fix β sufficiently small so that $-2b > g_S$. For this β, select k such that $g_S/2 < k < -b$. For this β and k, there exists T_0 sufficiently large such that whenever $T > T_0$, Π_{2T} has no fixed points and Π_T has exactly two fixed points, one of which is attracting.*

Remark 3.23 For example, $b = -1.5, \beta = 0.1$ gives $g_S \approx 2.15$, and the choice $k = 1.3$ and $T = 25$ gives a transition from non-recruitment to recruitment for $\Delta t \approx 45 < 2T$.

Proof: Note that b and θ_S are independent of β, k, T, all of which characterize the inputs to the cell, not its intrinsic dynamics. By taking β small, we can make g_S as close to $-b > 0$ as we wish, and in particular we can make $-2b > g_S$.

Recall from the one-input case that if $g_\tau^* < -b$ for some τ, then Π_τ has exactly two fixed points, an attracting one at $(\theta_1(g_\tau^*), g_\tau^*)$ and an unstable one at $(\theta_2(g_\tau^*), g_\tau^*)$. Further, θ_τ^* is bounded above by W^s and to the left by $\{\theta = \theta_S\}$, and the maximal g-coordinate of W^s on $\{(\theta, g) : \theta \geq \theta_S\}$ occurs at θ_S. Thus, if $g_\tau^* > g_S$, then Π_τ has no fixed points. Therefore, it suffices to show that for the selected β, we can choose k, T such that $g_T^* < -b$ and $g_{2T}^* > g_S$.

By our choice of β, it is possible to choose k such that $g_S/2 < k < -b$; fix k such that these inequalities hold. Now, $g_{2T}^* = 2k/(1 - e^{-2\beta T}) \to 2k$ as $T \to \infty$. Since $2k > g_S$,

$g^*_{2T} > g_S$ for T sufficiently large. Similarly, $g_T = k(1 + e^{-\beta T})/(1 - e^{-2\beta T}) \to k$ as $T \to \infty$, and since $k < -b$, it follows that $g^*_T < -b$ for T sufficiently large, as desired. □

3.4.2 Transition from non-recruitment to recruitment

For very large k, recruitment occurs for all Δt. The previous subsection shows that when k is not so large, $\theta^*_{\Delta t}$ exists, at least for some range of $g > 0$, for each $\Delta t \in [T, 2T]$. Further, $\theta^*_{\Delta t}$ varies from $\theta^*_{T \cup T}$ to θ^*_{2T} as Δt increases from T up to $2T$. The key to the transition from non-recruitment to recruitment, as Δt increases, is the change in location of $\theta^*_{\Delta t}$ relative to $g^*_{\Delta t}$. As in the IF case, equation (16) implies that $g^*_{\Delta t}$ increases with Δt, which would seem to promote recruitment. However, our numerics suggest that $\theta^*_{\Delta t}$ expands as Δt increases from T to $2T$, which would oppose recruitment. Indeed, unlike the IF case, where the curve $v^*_{\Delta t}(g)$ can first increase and then decrease as Δt increases, $\theta^*_{\Delta t}$ appears to expand monotonically. An example of this expansion appears in Figure 15, while Figure 16 shows a comparison of $\theta^*_{\Delta t}$ curves for different values of β with other parameters fixed.

Suppose that recruitment fails for $\Delta t = T$; that is, $\theta^*_{T \cup T}$ extends at least up to $g = g^*_T$, such that Π_T has a an attracting fixed point. As Δt increases, $g^*_{\Delta t}$ increases and $\theta^*_{\Delta t}$ expands, such that recruitment may or may not emerge. The opportunity for a transition to recruitment occurs at exactly those Δt values for which the maximum point of $\theta^*_{\Delta t}$ lies at $g = g^*_{\Delta t}$. If g^*_{2T} exceeds the maximum point of θ^*_{2T}, as Lemma 3.22 guarantees will occur for certain parameter choices, then recruitment certainly takes over for some $\Delta t < 2T$. Our results up to this point do not provide further information about this transition, but instead indicate which structures should be generated numerically to fill in the details of this transition for particular parameter sets.

A further example of these results, for β too large for Lemma 3.22 to apply, is illustrated in Figure 17. For the parameter values used, a unique transition from non-recruitment to recruitment does occur, at $\Delta t \approx 1.6 \in [T, 2T] = [1, 2]$, as can be seen in both panels of the figure. However, as Figure 17B emphasizes, $g^*_{\Delta t}$ lies very close to the saddle-node of $\theta^*_{\Delta t}$ for all Δt, in this example. Our simulations suggest that this is representative of a general effect in the θ model, namely that shifts in Δt lead to qualitatively similar shifts in $g^*_{\Delta t}$ and $\theta^*_{\Delta t}$. Hence, for wide ranges of parameters, the recruitment outcome is the same for all $\Delta t \in [T, 2T]$. This can be interpreted as a lack of sensitivity to Δt in the theta model, relative to the IF model, in which transitions from non-recruitment to recruitment with increasing Δt appear to be easier to achieve. This likely relates to the crucial role of Γ, which is independent of Δt, in the geometry of the IF model. Indeed, one can easily adjust Γ for the IF model, by adjusting the firing threshold v_{th}, such that small changes in Δt have a large effect. This type of control is not available in the θ model. In the θ model, the stable manifold W^s represents a Δt-

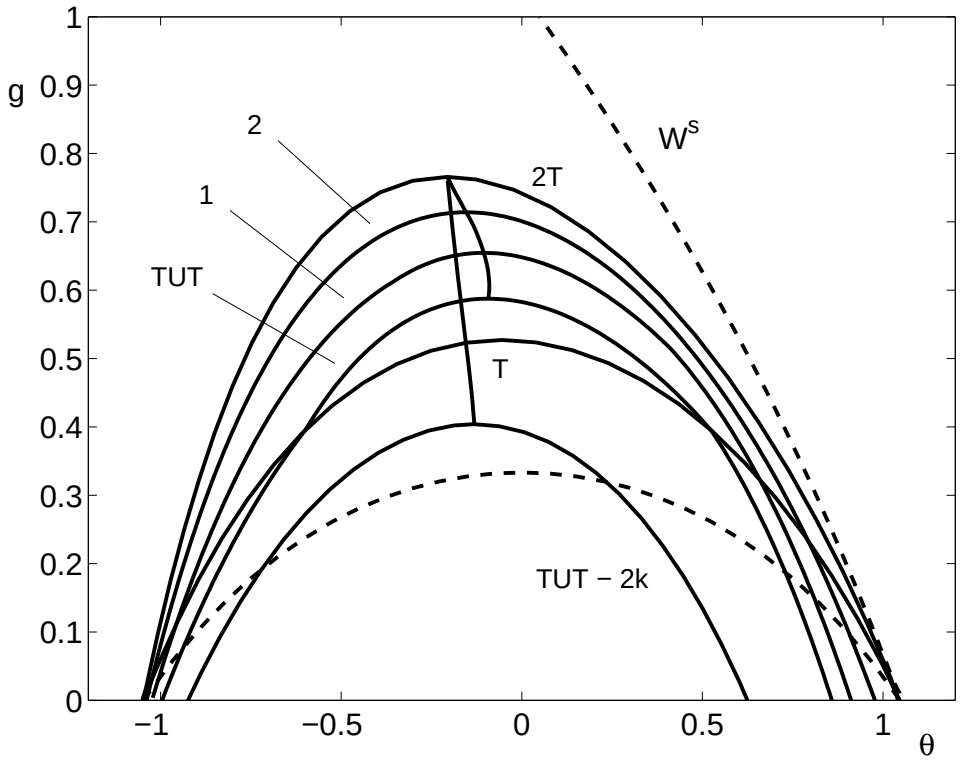

Figure 15: A collection of curves generated numerically from equations (5),(3),(4) with $b = -1/3$ and $\beta = 1$. The dashed curves are the θ-nullcline and the stable manifold of $(\theta_U, 0)$, labeled W^s. The main group of solid curves show $\theta^*_{\Delta t}$ for $k = 0.25$ and $\Delta t = T = 1$ (labeled T), $\Delta t = 1.5$ (labeled 1), $\Delta t = 1.8$ (labeled 2), and $\Delta t = 2T = 2$ (labeled 2T) as well as the limiting curve $\theta^*_{T\cup T}$ (labeled T $\cup$ T); note that $\theta^*_{T\cup T}$ and θ^*_T intersect at $g = g^*_T \approx 0.4$ and that $\theta^*_{\Delta t}$ expands as Δt increases. An additional solid curve connects from the saddle-node point of $\theta^*_{T\cup T}$ to that of θ^*_{2T}. Along this curve, g increases monotonically with Δt. The figure also shows $\theta^*_{T\cup T}$ for $k = 0.5$ (labeled T $\cup$ T - 2k), as well as the curve of saddle-nodes for $k = 0.5$, for comparison. Since θ^*_{2T} is independent of k, the $k = 0.25$ and $k = 0.5$ curves of saddle-nodes terminate at the same point.

independent structure that separates trajectories that cross threshold from those that do not, but the location of W^s cannot be changed independently from the locations of the other relevant geometric structures in the phase plane.

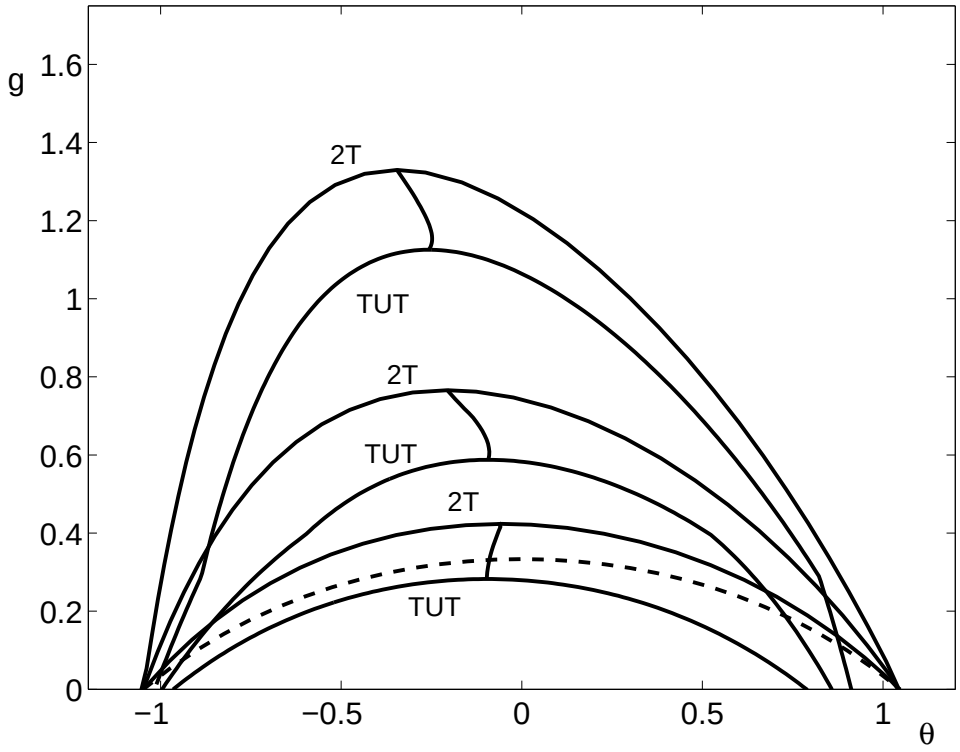

Figure 16: Extreme curves $\theta^*_{T\cup T}$ and θ^*_{2T} for $\beta = 0.25$ (smallest g), $\beta = 1$ (intermediate g), and $\beta = 2$ (largest g) with $b = -1/3$, $k = 0.25$, $T = 1$. Each pair is connected by the corresponding curve of saddle-nodes of $\theta^*_{\Delta t}$ for $\Delta t \in [T, 2T]$. The dashed curve shows the location of the θ-nullcline. Note that θ^*_{2T} asymptotes to $(\theta_S, 0)$ on one end and to $(\theta_U, 0)$ on the other, for all parameter choices.

4 Discussion

If a neuron is thought of as an integrator that sums its inputs, then the characteristics of its firing pattern reveal information about the types of inputs it receives. The most basic example one can consider is to see whether or not a neuron fires at all in response to a given set of inputs. In this paper, we have laid out a set of geometric criteria that allow us to determine whether or not a neuron will fire repeatedly in response to periodically delivered excitatory synaptic inputs, including pairs of inputs of differing degrees of synchrony. We called this process recruitment, in reference to ideas of pattern completion [14] or bump formation [6, 13].

In the context of both the integrate-and-fire (IF) and theta neuron models, we showed

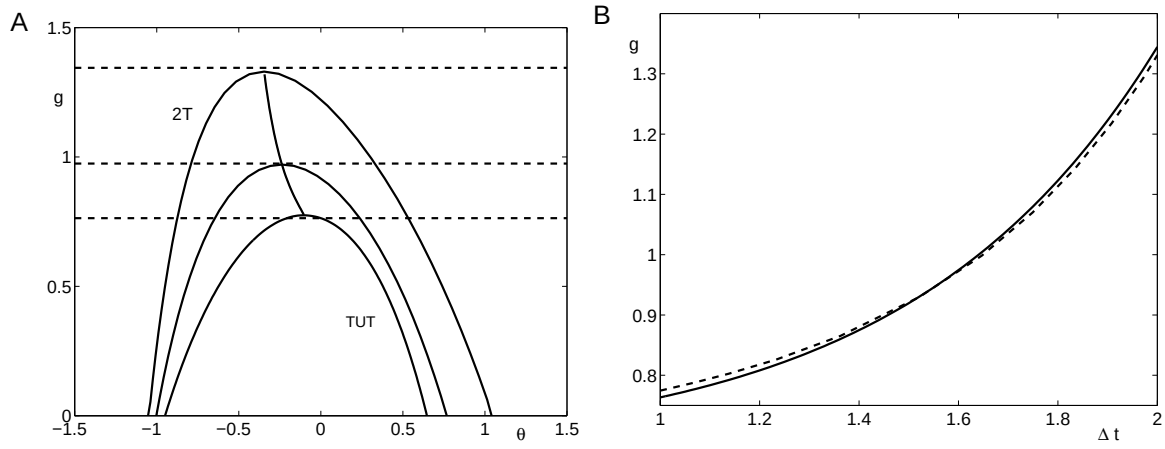

Figure 17: Transitions from non-recruitment to recruitment in the theta model can be subtle. This figure shows simulation results from equations (5),(3),(4) with $b = -1/3, \beta = 2$, and $T = 1$, as in Figure 16, but with $k = 0.66$. A) From lowest to highest, the solid curves are $\theta^*_{T\cup T}, \theta^*_{1.6}$, and θ^*_{2T}. The corresponding values of $g^*_{\Delta t}$ are dashed and the curve of saddle-nodes for $\Delta t \in [T, 2T]$ is also solid. The g^*_T line intersects $\theta^*_{T\cup T}$, corresponding to non-recruitment (which we verified in direct simulations). The g^*_{2T} line lies above θ^*_{2T}, corresponding to recruitment (again verified by simulation). The transition occurs very close to $\Delta t = 1.6$, as indicated by the proximity of the line $g^*_{1.6}$ to the maximum of $\theta^*_{1.6}$ and also verified in direct simulation. B) The curve of saddle-nodes plotted as g as a function of Δt (dashed) lies very close to the curve $g^*_{\Delta t}$ (solid). The former curve starts above the latter for $\Delta t = T = 1$, corresponding to non-recruitment, and intersects the latter uniquely near $\Delta t = 1.6$, yielding recruitment for all greater values of Δt.

that if the inputs to a neuron are sufficiently strong and frequent, occur in a sufficiently short time window (in the case of input pairs), and do not decay away too quickly, then recruitment of cells can occur. Our analysis shows how analytic calculations associated with the map P (IF case) or Π (theta case) relate to geometric constructs such as the exit set ES (IF case) or the set Θ (theta case). In particular, these structures allow us to establish precise geometric criteria in phase space that specify the transition between recruitment and non-recruitment as parameters are varied and that, for fixed parameter values, *a priori* determine whether or not a cells receiving the given inputs will be recruited. Interestingly, despite similarities in the IF and theta models, they feature qualitatively different geometries of the recruitment transition, which is given by a change in the location of a unique fixed point of P in the IF case and a change in the existence of fixed points of Π in the theta case. Note that this difference does not

simply correspond to the fact that the firing threshold is imposed arbitrarily in the IF model; although the location of the threshold affects the transition in IF, it does not change the existence of a unique fixed point of P.

The work that we presented here was motivated by trying to understand how regions of localized activity (bumps) are formed in purely excitatory networks [3, 17]. By clarifying what sets of inputs can or cannot recruit a cell into an activity pattern, we can analytically explain several observations that we made about bump formation in excitatory networks. Specifically, our results yield a condition on the degree of asynchrony between inputs that determines the boundary in parameter space between inputs that recruit cells and those that do not. When activity is initiated locally in a network and begins to spread, whether additional cells are recruited or not depends on the input they receive when the activity spreads close to them. Due to the gradual desynchronization of activity as it spreads in a network of excitatory Type I cells [4], different degrees of input synchrony will be present when activity reaches cells that are in different positions relative to the initially stimulated region. So our condition on input synchrony relates to which cells in the network will be recruited into a bump and which will not.

Our work also relates to the idea of synchrony-dependent propagation in feed forward networks [15]. Specifically, for activity to propagate from one layer to the next, there must be sufficient synchrony present in the inputs received by cells in the next layer, and our results make precise the degree of synchrony required, at least in the case of input pairs for IF and theta cells. Using firing rate measures of experimental data, Reyes showed that increased firing synchrony can occur in deeper layers of feed forward cortical networks, through a gradual enhancement of synchrony. Our work in this paper, applied to bump formation [17], gives insight into a parallel, but opposite, process. That is, we show how recruitment ends as synchrony breaks down, highlighting the consequences of the gradual loss of synchrony.

The work of Pakdaman [12] is very clearly related to our single input IF story, although we focus on the precise transition between recruitment and non-recruitment, whereas Pakdaman considered the evenutal firing pattern of recruited IF cells. Similarly, in other related work, Tiesinga derived analytic maps from the time of one spike to the time of the next, and he used these and simulations to study mode locking in the IF model. While Pakdaman's model incorporated a smooth T-periodic input $I(t)$ that changed signs on each period, such that $\int_0^T I(t)\,dt = 0$, Tiesinga [19] considered piecewise constant input that jumped between A and $-A$ either periodically or quasiperiodically, with or without noise. Both of these forms of input differ from our purely excitatory synaptic input with instantaneous onset. We did examine the firing patterns of cells driven with periodic trains of such synaptic input in a number of simulations of both the IF and theta neuron models, under various parameter combinations. The simulations suggest that when recruitment occurs in the IF case with one input per period, the solutions eventually lock to the stimulus and settle into periodicity. With two inputs

per period, solutions again appear to approach a periodic state, but we observe both phase-locking and phase drift, relative to the stimulus, depending on parameter values. The theta neuron case is harder to quantify, and details of firing patterns remain to be studied thoroughly.

Borgers and Kopell also have studied how excitable cells, including theta neurons, respond to different sets of synaptic inputs [1]. In this work, the authors concentrate on *E-I* networks in an attempt to understand the origins of the gamma rhythm in the hippocampus. They also state and prove some theorems on recruitment in the context of IF neurons, but their results focus on extreme cases of input synchrony or desynchrony, rather than transitions as the degree of input synchrony is varied, and their approach is less geometric than what we presented. Borgers and Kopell also discuss the existence of *rivers*, defined as certain strongly attracting or repelling trajectories. Rivers may very well play a role in the recruitment that we consider, since we often observe strong compression in simulations. Indeed, the lack of sensitivity to Δt in simulations of the 2-input theta model may very well relate to the strong compression of trajectories induced by the flow of equations (5),(3), although the details of such a relation remain to be determined. We find that the IF model can also yield strong compression, particularly below the v-nullcline. In IF, however, one can easily adjust the firing threshold v_{th} in a way that makes the cell more or less sensitive to Δt, a form of control that is not available in the θ model.

We have considered situations where the inputs to the excitable cell are identical. However, the ideas used here should generalize naturally to cases of many inputs, of unequal strengths and/or frequencies. The analysis would, of course, be much more complicated in such cases. However, the basic idea that the location of a fixed point of an appropriately defined map in the IF case, or the (lack of) existence of a fixed point in the theta neuron case, determines recruitment still holds in the more general setting. In other recent work, we have also begun studying how an excitable cell responds to stochastic inputs [18], using a Markov chain approach that yields firing statistics as a function of the interinput interval distribution. For each interinput interval in a stochastic train, the types of geometric structures discussed in this paper can be defined. However, the question of how to derive probabilistic statements relating recruitment likelihood to input train statistics remains for future work.

Acknowledgments. This work was partially supported by National Science Foundation grants DMS-0414023 (JR), DMS-0315862 (AB). We thank Bard Ermentrout for sharing XPPAUT tricks, on boundary value problems with resets, from his personal stash. We are also grateful for the hospitality of the Institute for Advanced Study/Park City Mathematics Institute, where a portion of this work was completed.

5 Appendices

5.1 Appendix A: The exit set $\tilde{ES}$ for IF with 2 inputs

A full exit set $\tilde{ES}$ for the case of two inputs is shown in Figure 18. Note that depending on parameters, $\tilde{ES}$ may look as shown in the figure or slightly differently as described below.

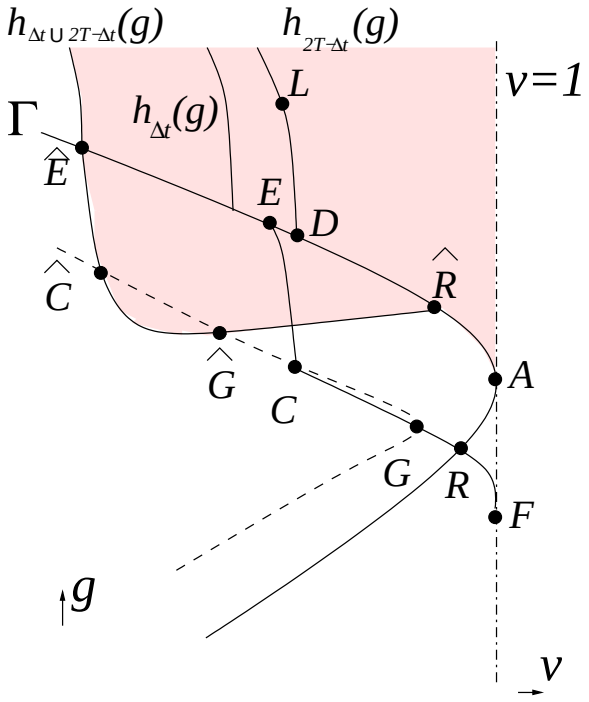

Figure 18: The shaded region indicates the full exit set $\tilde{ES}$ for the 2-input case. Initial conditions that lie in this region are mapped into the set $\{v > 1\}$ in time less than or equal to $2T$. See the text for definition of labeled points.

The points A and R are previously defined, but we repeat their definitions and define other points here. A is the point along the v-nullcline that intersects the threshold $\{v = 1\}$. The curve Γ is the forward and backward trajectory through A. The point D, along Γ, is obtained by flowing A backward a time $2T - \Delta t$. The point R is the unique point of intersection of Γ and the curve obtained by shifting Γ down by k units in the g-direction. The curve $h_{2T-\Delta t}(g)$ contains points that are exactly $2T - \Delta t$ away from threshold and lies to the right of $h_{\Delta t}(g)$ since $2T - \Delta t < \Delta t$. The point L lies along the curve $h_{2T-\Delta t}(g)$ and is k units above Γ. The points E, C and F lie k units below

L, D and A, respectively, as shown in Figure 18. Any point in the region $ECRADE$, if synaptically reset, will be placed in the region above Γ and to the right of $h_{2T-\Delta t}(g)$. Thus these points are less than $2T - \Delta t$ away from the threshold and, when flowed forward, will cross threshold before time $2T$. Therefore, to understand what points are in the full exit set $\tilde{ES}$, we need to understand what points flow into this region in time Δt.

Consider the forward trajectory through C (the forward and backward trajectory through C is dashed in Figure 18). If the magnitude of the vector field through this point is less than the magnitude of the slope of the curve CRF at the point C, then the forward trajectory must intersect the curve CRF at a point, labeled G in Figure 18. The points $\hat{C}$, $\hat{E}$, $\hat{G}$ and $\hat{R}$ are obtained by flowing C, E, G and R, backwards in time Δt, respectively. The set of points contained within the region $\hat{E}\hat{C}\hat{G}\hat{R}\hat{E}$, when flowed forward time Δt, yields the region $ECRADE$. Thus points in $\hat{E}\hat{C}\hat{G}\hat{R}\hat{E}$ lie no more than $2T$ away from threshold (keeping synaptic reset in mind), and are therefore part of $\tilde{ES}$. Note that, as shown in Figure 18, the part of the boundary of $\hat{E}\hat{C}\hat{G}\hat{R}\hat{E}$ between $\hat{C}$ and $\hat{G}$ extends below the trajectory from $\hat{C}$ to $\hat{G}$ in this case. The points on this boundary segment are exactly those points that flow to the segment CG of the curve CRF in time Δt.

The subset of $\tilde{ES}$ described above results when the condition on slopes at the point C is met. This can occur, for example, if β is small and there is much greater contraction in the v-direction than in the g-direction. When the slopes at the point C do not meet the condition outlined above, then the point G does not exist and the ensuing full exit set would contain a region bounded by just $\hat{E}\hat{C}\hat{R}\hat{E}$.

A second portion of $\tilde{ES}$ lies above Γ and is easier to understand. Points along the curve $h_{\Delta t \cup 2T-\Delta t}(g)$, when flowed forward for time Δt, are reset to points above L on the curve $h_{2T-\Delta t}(g)$. Thus, any points lying on or to the right of $h_{\Delta t \cup 2T-\Delta t}(g)$ are no more than $2T$ away from threshold, with reset at Δt taken into account, and are also part of $\tilde{ES}$.

5.2 Appendix B: Refinement of the possible recruitment progression with Δt for IF with 2 inputs

In this appendix, we establish some results that refine the picture of how the progression from non-recruitment to recruitment may or may not occur as Δt is increased in the interval $[T, 2T]$. Note that for every $\Delta t \in [T, 2T]$, there exists a unique g such that $(v^*_{\Delta t}(g), g) \in \Gamma$. Also, recall that $\hat{\Gamma}_{\Delta t}$ denotes the part of Γ lying between $\hat{R}_{\Delta t}$ and Q.

Lemma 5.1 *Suppose that $(v^*_{\Delta t}(g), g) \in \Gamma \setminus \hat{\Gamma}_{\Delta t}$. If $(v^*_{\Delta t}(g), g)$ lies in the part of Γ that is to the left of $\hat{\Gamma}_{\Delta t}$, then $g > g^*_{\Delta t}$, while if $(v^*_{\Delta t}(g), g)$ lies in the part of Γ that is to the right of $\hat{\Gamma}_{\Delta t}$, then $g < g^*_{\Delta t}$.*

Proof: If $(v^*_{\Delta t}(g), g)$ lies to the left of $\hat{\Gamma}_{\Delta t}$, then the argument used to prove Lemma 3.9 implies that $g(2T^+) < g(0^+)$. Hence, $g > g^*_{\Delta t}$. Similarly, if $(v^*_{\Delta t}(g), g)$ lies to the right of $\hat{\Gamma}_{\Delta t}$, then the argument used to prove Lemma 3.11 implies that $g(2T^+) > g(0+)$. Hence, $g < g^*_{\Delta t}$. □

The following lemma gives a necessary condition for recruitment to occur for some $\Delta t \in (T, 2T]$, given that it does not occur for $\Delta t = T$.

Lemma 5.2 *If recruitment fails for $\Delta t = T$ but occurs for any $\Delta t \in (T, 2T]$, then the point $p_1 \equiv \hat{R}_{2T} \in \Gamma$ lies to the left of the point $p_2 \equiv v^*_{2T}(g) \cap \Gamma$.*

Proof: Let $p_i = (v_i(0), g_i(0))$ for $i = 1, 2$ and suppose to the contrary that p_2 lies to the left of p_1, such that $v_2(0) < v_1(0)$. Then the flow of system (2)-(3) for time $2T$, with initial conditions $(v_i(0), g_i(0))$, gives $v_1(0) > v_2(0) = v_2(2T) > v_1(2T) = v_Q$, such that Q is to the left of $\hat{R}_{2T}$. Since $\hat{R}_{\Delta t}$ moves to the left along Γ as Δt increases, while Q is fixed, this implies that Q is to the left of $\hat{R}_{\Delta t}$ for all $\Delta t \in [T, 2T]$. Therefore, by Lemma 3.10, it follows that for all $\Delta t \in [T, 2T]$, the fixed point of $P_{\Delta t}$ lies outside of Γ, and hence a transition from non-recruitment to recruitment cannot occur as Δt increases from T, a contradiction. □

Putting together 5.1 with 5.2, the transition from non-recruitment with $\Delta t = T$ to recruitment with $\Delta t = 2T$, if it occurs, must occur as follows. When $\Delta t = T$, the fixed point (v^*_T, g^*_T) of P_T lies outside of ES, while $v^*_T(g) \cap \Gamma$ lies to the left of at least one of $\hat{R}_T$ and Q. As Δt increases, eventually $\hat{R}_{\Delta t}$ must lie to the left of Q, and a transition is reached at a value Δt_c at which the fixed point $(v^*_{\Delta t_c}, g^*_{\Delta t_c})$ of $P_{\Delta t_c}$ lies in $\hat{\Gamma}_{\Delta t_c} \subset \Gamma$. If the transition is unique, then for each $\Delta t > \Delta t_c$, the point $v^*_{\Delta t}(g) \cap \Gamma$ must remain to the right of $\hat{R}_{\Delta t}$. See Figure 6 for an illustration of an example of this progression. Note, however, that we have not yet ruled out multiple transitions between recruitment and non-recruitment.

5.3 Appendix C: The expression for $\hat{g}_{\Delta t}$ for IF with 2 inputs

To derive an expression for $\hat{g}_{\Delta t}$, recall that $Q = (v_Q, g_Q)$ is the point on Γ that has the same v-coordinate as $R \in \Gamma$ but lies above the v-nullcline. That is, R gets reset to Q. We start by deriving the expression for g_Q.

Let $c = (I - 1)/(1 - E)$ denote the g-coordinate of the point A, where Γ intersects both $v = 1$ and the v-nullcline, from equation (7). Note that the time for g_Q to decay to c is $\tilde{t} = -(1/\beta)\ln(c/g_Q)$ by equation (3). Thus, $\tilde{t}$ is a function of g_Q. Based on this, we can derive an expression for v_Q as a function of g_Q by integrating equation (2) for time $\tilde{t}$, with $v(0) = v_Q$ and $v(\tilde{t}) = 1$. We omit writing out this expression here.

Next, we note that the time for g_Q to decay to $g_Q - k$ is

$$t = -(1/\beta)\ln(1 - k/g_Q), \tag{27}$$

where clearly $g_Q > k$ by definition. Also by definition, if we integrate equation (2) for time t, with $v(0) = v_Q$, then we obtain $v(t) = v_Q$ as well. Using this, we obtain an equation linking v_Q with t, which is effectively a second equation relating g_Q with t, since v_Q is a function of g_Q. Combining this equation with equation (27) yields the following equation to be solved for g_Q, depending on the fixed parameters β, k, E, and I,

$$\int_0^{-\frac{1}{\beta}\ln(1-\frac{k}{g_Q})} h(g_Q, s)\, ds = \left[\left(\frac{g_Q}{g_Q - k}\right)^{1/\beta} e^{\frac{k}{\beta}} - 1\right]\left[\left(\frac{g_Q}{c}\right)^{1/\beta} e^{-\frac{c}{\beta}}(1 - I) - \int_0^{-\frac{1}{\beta}\ln(1-\frac{c}{g_Q})} h(g_Q, s)\, ds\right], \tag{28}$$

where $h(g_Q, s) = E_1 g_Q e^{-\beta s} e^{s - \frac{g_Q}{\beta} e^{-\beta s}}$.

Finally, we obtain $\hat{g}_{\Delta t}$ by flowing from (v_Q, g_Q) backward in time an amount $\Delta t - t$, if $\Delta t > t$, or forward an amount $t - \Delta t$, if $\Delta t < t$. Given that $t = -(1/\beta)\ln(1 - k/g_Q)$ from equation (28), this yields $\hat{g}_{\Delta t} = g_Q e^{\beta \Delta t}(1 - k/g_Q)$.

References

[1] C. Börgers and N. Kopell. Effects of noisy drive on rhythms in networks of excitatory and inhibitory neurons. *Neural Comp.*, **17**:557–608, 2005.

[2] C. Carr and M. Konishi. A circuit for detection of interaural time differences in the brain stem of the barn owl. *J. Neurosci.*, **10**:3227–3246, 1990.

[3] J. Drover and B. Ermentrout. Nonlinear coupling near a degenerate Hopf (Bautin) bifurcation. *SIAM J. Appl. Math.*, **63**:1627–1647, 2003.

[4] B. Ermentrout. Type I membranes, phase resetting curves, and synchrony. *Neural Comput.*, **8**:979–1001, 1996.

[5] B. Ermentrout. *Simulating, Analyzing, and Animating Dynamical Systems.* SIAM, Philadelphia, 2002.

[6] G. Ermentrout. Neural nets as spatio-temporal pattern forming systems. *Reports on Progress in Physics*, **61**:353–430, 1998.

[7] G. Ermentrout and N. Kopell. Parabolic bursting in an excitable system coupled with a slow oscillation. *SIAM J. Appl. Math.*, **46**:233–253, 1986.

[8] F. Hoppensteadt and E. Izhikevich. *Weakly Connected Neural Networks*. Springer-Verlag, New York, Berlin, and Heidelberg, 1997.

[9] J. P. Keener, F. C. Hoppensteadt, and J. Rinzel. Integrate-and-fire models of nerve membrane response to oscillatory input. *SIAM J. Appl. Math.*, **41**(3):503–517, 1981.

[10] N. Kopell and G. Ermentrout. Subcellular oscillations and bursting. *Math. Biosci.*, **78**:265–291, 1986.

[11] C. Morris and H. Lecar. Voltage oscillations in the barnacle giant muscle fiber. *Biophys. J.*, **35**:193–213, 1981.

[12] K. Pakdaman. Periodically forced leaky integrate-and-fire model. *Phys. Rev. E*, **63**:041907–1 – 041907–5, 2001.

[13] D. Pinto and G. Ermentrout. Spatially structured activity in synaptically coupled neuronal networks: II. Lateral inhibition and standing pulses. *SIAM J. Appl. Math*, **62**:226–243, 2001.

[14] M. Recce. Encoding information in neuronal activity. In W. Maass and C. Bishop, editors, *Pulsed Neural Networks*, pages 111–132. MIT Press, 1998.

[15] A. Reyes. Synchrony-dependent propagation of firing rate in iteratively constructed networks *in vitro*. *Nat. Neurosci.*, **6**:593–599, 2003.

[16] J. Rinzel and G. Ermentrout. Analysis of neural excitability and oscillations. In C.Koch and I. Segev, editors, *Methods in Neuronal Modeling: From Ions to Networks*, pages 251–291. The MIT Press, Cambridge, MA, second edition, 1998.

[17] J. Rubin and A. Bose. Localized activity patterns in excitatory neuronal networks. *Network: Comput. Neural Syst.*, **15**:133–158, 2004.

[18] J. Rubin and K. Josić. The firing of an excitable neuron in the presence of stochastic trains of strong synaptic inputs, 2005. submitted.

[19] P. Tiesinga. Precision and reliability of periodically and quasiperiodically driven integrate-and-fire neurons. *Phys. Rev. E*, **65**:041931–0419314, 2002.

[20] X.-J. Wang. Synaptic reverberation underlying mnemonic persistent activity. *Trends Neurosci.*, **24**:455–463, 2001.